frontiers | Frontiers in Earth Science

TYPE Original Research
PUBLISHED 15 May 2024
DOI 10.3389/feart.2024.1359157

OPEN ACCESS

EDITED BY
Marta Rodrigo-Gámiz,
University of Granada, Spain

REVIEWED BY
Josef Werne,
University of Pittsburgh, United States
Antonio Garcia-Alix,
University of Granada, Spain

*CORRESPONDENCE
Nicolò Ardenghi,
nicolo.ardenghi@gmail.com

RECEIVED 20 December 2023
ACCEPTED 21 March 2024
PUBLISHED 15 May 2024

CITATION
Ardenghi N, Mulch A, McFarlin JM, Sachse D, Kahmen A and Niedermeyer EM (2024), Leaf wax *n*-alkane distribution and hydrogen isotopic fractionation in fen plant communities of two Mediterranean wetlands (Tenaghi Philippon, Nisí fen—Greece). *Front. Earth Sci.* 12:1359157. doi: 10.3389/feart.2024.1359157

Leaf wax *n*-alkane distribution and hydrogen isotopic fractionation in fen plant communities of two Mediterranean wetlands (Tenaghi Philippon, Nisí fen—Greece)

Nicolò Ardenghi[1]*, Andreas Mulch[1,2], Jamie M. McFarlin[3], Dirk Sachse[4], Ansgar Kahmen[5] and Eva M. Niedermeyer[1]

[1]Senckenberg Biodiversity and Climate Research Centre (SBiK-F), Frankfurt, Germany, [2]Institute of Geosciences, Goethe University Frankfurt, Frankfurt, Germany, [3]Department of Geology and Geophysics, University of Wyoming, Laramie, WY, United States, [4]GFZ German Research Centre for Geosciences, Potsdam, Germany, [5]Department of Environmental Sciences, University of Basel, Basel, Switzerland

Many continental paleoclimate archives originate from wetland sedimentary sequences. While several studies have investigated biomarkers derived from peat-generating vegetation typical of temperate/boreal bogs (e.g., *Sphagnum*), only scant information is available on emergent plants predominant in temperate/subtropical coastal marshlands, peri-lacustrine and fen environments. Here, we address this gap, focusing on two wetlands in the Mediterranean (Nisí fen and Tenaghi Philippon, Greece). We examined the concentration, homologue distribution, and hydrogen stable isotopic composition (δ^2H) of leaf wax *n*-alkanes in 13 fen plant species, their surrounding soil, and surface water during the wet growing season (spring) and the declining water table period (summer). Our findings indicate that local graminoid species primarily contribute to the soil *n*-alkane signal, with a lesser influence from forbs, likely owing to differences in morphology and vegetation structure. The δ^2H values of surface and soil water align with local average annual precipitation δ^2H, reflecting winter-spring precipitation. Consistently, the average δ^2H of local surface, soil, and lower stem water showed negligible evaporative enrichment, confirming minimal ^{2}H-fractionation during water uptake. We find that δ^2H values of source water for wax compound synthesis in local fen plants accurately mirror local annual precipitation. Furthermore, despite differences between leaves and lower stems in *n*-alkane production rates, their δ^2H values exhibit remarkable similarity, indicating a shared metabolic substrate, likely originating in leaves. Our net ^{2}H-fractionation values (i.e., precipitation to leaf *n*-alkanes) align with those in Chinese highlands and other similar environments, suggesting consistency across diverse climatic zones. Notably, our data reveal a seasonal decrease in the carbon preference index (CPI) in plant samples, indicating wax lipid synthesis changes associated with increased aridity. Additionally, we introduce a new parity isotopic difference index (PID) based on the consistent δ^2H difference between odd and even *n*-alkane homologues. The PID demonstrates a strong anticorrelation with plant CPI, suggesting a potential avenue to trace long-term aridity shifts through

δ^2H analysis of odd and even *n*-alkane homologues in sedimentary archives. While further development of the PID is necessary for broad application, these findings highlight the intricate interplay between plant physiology, environmental parameters, and sedimentary *n*-alkanes in unravelling past climatic conditions.

KEYWORDS

***n*-alkanes, hydrogen isotopes, fractionation, Mediterranean wetland, Tenaghi Philippon, emergent plants, parity isotopic difference, leaf wax synthesis**

Highlights

- Soil *n*-alkane signal mainly determined from C_3 graminoids, particularly leaves;
- Alignment of δ^2H values of surface, soil, lower stem water, and annual precipitation, confirm the potential of local plant communities to trace long-term seasonality shifts;
- Similar δ^2H values of wax compounds in leaves and lower stems suggest a common metabolic substrate, likely originating in leaves;
- Net ^2H-fractionation values align with studies in Chinese highlands, suggesting a consistent signal in peri-lacustrine/fen communities;
- Seasonal plant CPI shift indicates *n*-alkane synthesis changes linked to increased aridity;
- New odd/even-numbered *n*-alkanes δ^2H difference index (PID) shows promise as a potential proxy for tracing long-term qualitative aridity shifts

1 Introduction

n-Alkanes are common components of epicuticular leaf waxes, which provide protection against mechanical damage and help regulating evapotranspiration (e.g., Eglinton and Hamilton, 1967; Koch and Ensikat, 2008). Owing to their covalent C-H bonds and absence of functional groups, *n*-alkanes exhibit remarkable resistance to degradation, allowing their preservation in sediments for millions of years (Eglinton and Logan, 1991). Their distribution of homologues can be source-specific, with different plant forms peaking at longer or shorter chain lengths. Additionally, their stable isotopic composition (δ^2H and $\delta^{13}C$) can offer valuable insights into environmental conditions, such as precipitation δ^2H, or differentiate between plant types (e.g., C_3 vs. C_4 plants) at the time of plant growth (e.g., Schefuß et al., 2003; Chikaraishi et al., 2004b; Sachse et al., 2004b; Feakins and Sessions, 2010; Freimuth et al., 2017). As a result, sedimentary plant waxes serve as valuable proxies for paleoclimate reconstructions, providing different information on past vegetation dynamics and hydroclimate (Jansen and Wiesenberg, 2017). However, plant *n*-alkane properties are highly responsive not only to changes in climatic-environmental parameters, but also to variations in plant types, morphology, and physiology. Consequently, regional studies on *n*-alkanes synthesis, occurrence, and deposition within contemporary plant communities play a pivotal role in refining the interpretation of sedimentary *n*-alkanes in downcore records.

1.1 Objectives

Here we focus on the (1) *n*-alkane abundance and distributions and (2) *n*-alkane and internal water ^2H-composition of several species of helophytes (i.e., emergent plants such as reeds, sedges, etc.) that make up the dominant vegetation in two Greek wetland sites (Kalaitzidis, 2007).

In the last two decades, the qualitative interpretation of *n*-alkane distribution and *sed*-δ^2H_{wax} has been frequently employed to infer past environmental shifts and develop paleo-hydrological reconstructions (e.g., Sachse et al., 2004a; Collins et al., 2013; Niedermeyer et al., 2016a; Tierney et al., 2017; Ardenghi et al., 2019; Butiseacă et al., 2022). In this context, several studies provided insight on the controls on *n*-alkane distribution and δ^2H_{wax} of various plant communities in different environments and climates (Diefendorf and Freimuth, 2017; Liu and An, 2018 and refs therein). While a number of plant wax studies have investigated wetland vegetation such as at the Gannan Gahai lake or the Dajiuhu peatland in China (trees, grasses and aquatics; Duan et al., 2014; Zhao et al., 2018; Huang and Meyers, 2019), British coastal salt marshes (mainly halophytes; Eley et al., 2014, 2018) or high latitude bogs (Ficken et al., 1998; Pancost et al., 2002; Nichols et al., 2006, 2010; Brader et al., 2010), none to date focus specifically on the helophytic plant communities so common worldwide in temperate fens, marshes, and peri-lacustrine environments (e.g., Silliman and Schelske, 2003; Mead et al., 2005), from which derive a great number of continental paleo-archives (e.g., Fischer and Wilkes, 2003; Kaufman et al., 2020).

Especially in the Mediterranean region, where alkaline fens are characterised by the predominance of reeds such as sedges (Cyperaceae) and grasses (Poaceae) and absence of mosses (*Sphagnum*; Britton and Crivelli, 1993; Raeymaekers, 1998; Hajek et al., 2006; Tanneberger et al., 2017; Pontevedra-Pombal et al., 2019), these communities often produce sedimentary sequences (e.g., peat) that become valuable climate archives (e.g., Carrión and Van Geel, 1999; Mighall et al., 2006; Desprat et al., 2013; Pross et al., 2015).

In addition, studying the *n*-alkane properties of plants in these Mediterranean marshes has a particular paleo-climatic relevance due to the peculiar seasonality of Mediterranean geography and climate. Typically, due to changes between winter and summer atmospheric configuration (Xoplaki et al., 2003; Lionello et al., 2014) Mediterranean precipitation originates either locally (less ^2H-depleted), mostly in summer, or from the Atlantic (more ^2H-depleted) during the rest of the year (IAEA/WMO, 2017; Hellenic National Meteorological Service, 2018).

Factors like light availability, temperature, and the characteristic summer aridity (Vilà and Sardans, 1999; Peichl et al., 2018), roughly constrain the timing of the growing season between spring and summer. This transitional period is very sensitive to long term changes in seasonality, especially drought, which can greatly affect the δ^2H of regional fresh water bodies (Dotsika et al., 2010) including, likely, the topogenous, karstic fed mires selected as our study sites. This means that major changes in atmospheric circulation in this region would likely translate into seasonality shifts, affecting the growing season of the local plant community in two main ways. First, changes in moisture levels would impact evapo-transpiration and drought-related stress mechanisms, which would likely be reflected in shifts in the production and distribution of plant *n*-alkanes as well as in their net ^2H-fractionation. Second, the balance of moisture sources (Mediterranean vs. Atlantic) would be significantly altered, impacting the δ^2H of source water available to plants, and thus, potentially, of their leaf waxes. Local fen plant communities can thus potentially serve as valuable recorders of long-term seasonality shifts, which could then be historically reconstructed from the resulting sedimentary archives (Ardenghi et al., 2019; Dixit et al., 2019).

Through this study we attempt to increase our understanding of the *n*-alkane environmental controls and ^2H-fractionation mechanisms of these helophytic communities, as well as ascertaining the ^2H-composition of their source water and its relation to the ^2H-composition of precipitation. Our aim is to improve the interpretation of sedimentary *n*-alkane distribution and ^2H-composition (*sed*-δ^2H_{wax}) primarily in such archives, and, secondarily, in any environment where these types of plants provide an important share of sedimentary waxes.

1.2 *n*-Alkanes as biomarkers

1.2.1 Distribution

Various plant species and communities exhibit distinct patterns of *n*-alkane homologues, tipically characterised by a pronounced odd-over-even predominance, while most bacteria and few plant species preferentially produce even carbon numbered homologues (Dembicki et al., 1976 and refs. therein).

The shortest homologues ($<C_{21}$, typically C_{17}) are commonly associated with bacteria and algae (Han and Calvin, 1969; Arp et al., 1999; Sachse and Sachs, 2008; Chatterjee et al., 2023). *Sphagnum spp.* (C_{23}; Nott et al., 2000) and aquatic plant chain lengths tend to peak at C_{21-25}, in contrast to terrestrial plants, which often that peak at C_{27-33} (Cranwell et al., 1987; Ficken et al., 2000; Gao et al., 2011; Bush and McInerney, 2013; Liu H. et al., 2019), although recent research challenges this dichotomy (e.g., Stefanescu et al., 2023).

Among terrestrial plants, trees/shrubs typically exhibit maximum abundances at C_{27-29} while grasses show a predominance of C_{31} (Cranwell, 1984; Meyers, 2003; Struck et al., 2020). While broad observations suggest that the average chain length (ACL) correlates with temperature/aridity-driven changes in production preferences along environmental gradients, different plant species may exhibit opposing behaviours (Hoffmann et al., 2013; Tipple and Pagani, 2013; Bush and McInerney, 2015; Teunissen van Manen et al., 2019).

Although ACL differences have been employed to discriminate among plant groups in particular environments (e.g., distinguishing gymnosperms/angiosperms and monocots/dicots on the Chinese Loess plateau; Liu et al., 2018), no definitive universally applicable correlation of ACL to plant groups has been established to date (e.g., Bush and McInerney, 2013). Recent studies emphasize the need to complement ACL and other indices (e.g., aquatic plant index) with additional other indicators (e.g., ^{13}C-composition of *n*-alkanes) to effectively distinguish sources among submersed, floating, and emergent plants (e.g., Yu et al., 2021).

1.2.2 Stable isotopic composition

The hydrogen isotopic composition of leaf wax *n*-alkanes (δ^2H_{wax}) from modern plants has been found to generally correlate with the δ^2H value of the plant source water, which often reflects precipitation δ^2H (δ^2H_p; e.g., Sessions et al., 1999; Sauer et al., 2001; Sachse et al., 2004b). In fact, the δ^2H_{wax} values from modern sedimentary wax compounds globally also robustly record local δ^2H_p values (Ladd et al., 2018; Liu and An, 2019; McFarlin et al., 2019). On this basis, the δ^2H of sedimentary *n*-alkanes, particularly of their C_{29} and C_{31} homologues, recovered both in marine and continental cores as well as in biologically reworked deposits (e.g., mammals' middens; Chase et al., 2019), has been used as a tracer for paleo-precipitation isotopic composition (e.g., Sachse et al., 2004a; Niedermeyer et al., 2014, 2016b; Tierney et al., 2017; Ardenghi et al., 2019). The accuracy of δ^2H_{wax} and chain length distribution as paleo-climate indicators relies on the understanding of *n*-alkane synthesis and of the influence and interaction of several internal (plant physiology) and external (environmental) variables.

As *n*-alkanes retain the δ^2H values established at the time of biosynthesis (Sachse et al., 2012), the average δ^2H_{wax} of single leaves can be biased toward growth water values available at the early stages of leaf growth (Sachse et al., 2010, 2015; Tipple et al., 2013; Tipple and Pagani, 2013; Gamarra and Kahmen, 2017). This may be caused by the timing of leaf synthesis (e.g., early growth often relies on synthates stored at the end of the previous year; Gao et al., 2015; Newberry et al., 2015; Freimuth et al., 2017) and, more generally, changes in the biosynthetic water pool linked to external factors such as temperature and relative humidity (Hou et al., 2008; Kahmen et al., 2008; Zhou et al., 2011; Douglas et al., 2012; Gao et al., 2014b; Bai et al., 2019; Jacob et al., 2021; Eensalu et al., 2023), light intensity (Yang et al., 2009), salinity (Ladd and Sachs, 2012; He et al., 2017; Ceccopieri et al., 2021; Wang et al., 2022), seasonality (Sessions, 2006; Pedentchouk et al., 2008; Kahmen et al., 2011; Newberry et al., 2015; Liu et al., 2017), elevation (e.g., Pérez-Angel et al., 2022) and precipitation δ^2H (δ^2H_p; Sachse et al., 2006, 2010, 2012; Liu and Yang, 2008; Rao et al., 2009; Feakins and Sessions, 2010).

Internal factors, linked to plant physiology (e.g., biosynthetic pathway, rooting depth) can also contribute to the variation in δ^2H_{wax} (Smith and Freeman, 2006; Gao et al., 2015; Cormier et al., 2018, 2019; Eley et al., 2018) and modulate the correlation between δ^2H_p and δ^2H_{wax}, normally expressed as the net (or apparent) ^2H-fractionation between *n*-alkanes and mean annual precipitation (e.g., $\varepsilon_{29/MAP}$) (Liu et al., 2006, 2016; Hou et al., 2007b; Sachse et al., 2012; Gao et al., 2014a; Gamarra et al., 2016; Eley et al., 2018). Despite the resulting high inter- and intra-specific variability

characterising δ^2H_{wax} (e.g., 40‰ between leaves of the same plant; Sachse et al., 2009; Newberry et al., 2015), larger datasets reveal a generally stable correlation between δ^2H_{wax} and δ^2H_p in plant communities and derived sediments (Chikaraishi and Naraoka, 2003; Sachse et al., 2006; Hou et al., 2008; Rao et al., 2009; Feakins and Sessions, 2010; Chen et al., 2022). Recent interpretive structural modelling has grouped and hierarchically classified multiple controlling factors such as δ^2H_p, evapotranspiration, and plant types, according to their relative impact on δ^2H_{wax} variability (Liu and An, 2018).

2 Methods

2.1 Approach

In order to investigate seasonal and species-specific differences characterising the plant communities building these sedimentary archives, we sampled several species of emergent plants from two climatically similar sites in northern Greece during the summer (dry season) of 2014 and the following spring (wet growing season). We analysed the abundance and distribution of *n*-alkanes in leaf, lower stem, and sub-surface soil samples, as well as the hydrogen isotopic composition of (1) water from soil, lower stems, and leaves, and of (2) *n*-alkanes extracted from leaves and lower stems.

2.1.1 Sampling sites

For this work we selected two sampling sites (Figure 1): one, the Tenaghi Philippon (TP) peatland in NE Greece (Figures 1, 2A), is the site of a historical permanent large wetland, recently (1930s) converted to farmland, as well as the site of important sedimentary paleoclimate archive (e.g., Wijmstra, 1969; Tzedakis et al., 2006; Pross et al., 2015; Schemmel et al., 2016; Ardenghi et al., 2019), and one, the Nisí fen, is a relatively undisturbed permanent-seasonal marshland at the Edessaios river's source in NW Greece (Figures 1, 2B) and a good ecological analogue for the original TP environment (Kalaitzidis, 2007). Both the original TP marshland and Nisí fen are examples of topogenous mesotrophic mires (i.e., mires that are predominantly fed by local karstic aquifers) situated in the lowest areas of intra-mountainous basins. The two sites share similar basic climatic parameters (temperature, precipitation; Table 1) and the same Köppen-Geiger climate classification (Csa, i.e., warm temperate with arid, hot summers; Kottek et al., 2006) with localised humid conditions during most of the year, and occasional frost episodes, due to thermal inversion and cold bursts from the northern mountain chains, punctuating the relatively mild and wet winters (Christanis, 1994; Pross et al., 2015; Hellenic National Meteorological Service, 2018).

The TP peatland is the result of millions of years of accumulation of Cyperaceae and other peat-forming helophytes in what once was a fen environment characterised by alkaline conditions (Kalaitzidis, 2007). The original wetland was almost completely drained in the 1930s, resulting also in the alteration of its natural water regime. However, stable residual pockets of helophytic communities survive in areas along the draining canals. Circa 16% of the samples were collected from these areas, in an effort to provide a basis for direct data comparison between TP and the mostly undisturbed Nisí fen site.

2.1.2 Species

We selected six species of widespread perennial monocots: the C_3 graminoids *Carex riparia* (greater pond sedge), *Cladium mariscus* (saw-sedge), *Phragmites australis* (common reed), *Typha angustifolia* (narrowleaf cattail) and *Scirpus lacustris* (common club-rush), and the C_4 graminoid *Cyperus longus* (galingale). We focused on helophytes, firstly graminoids, as they have a preeminent role in the formation of peat deposits in these types of marshlands, which often produce important paleoclimatic archives (e.g., Miola et al., 2006; Borromei et al., 2010; Chawchai et al., 2015; Pross et al., 2015) and are not *Sphagnum* dominated such as acidic (e.g., *Carex* and *Cladium* are phylo-calcareous genera; Buczek, 2005; Theocharopoulos et al., 2006) peat-forming oligotrophic bogs (Anderson et al., 2013).

To cover a broader range of wetland species and plant forms, we sampled a group of five perennial eudicot species, the C_3 forbs *Cirsium palustre* (swamp thistle, biennial/perennial), *Stachys palustris* (marsh woundwort), *Mentha aquatica* (water mint), *Lythrum salicaria* (purple loosestrife), *Galium uliginosum* (fen bedstraw), as well as the C_3 pteridophyte *Equisetum fluviatile* (water horsetail) and the C_3 the perennial basal angiosperm *Nymphaea alba* (white water lily, a rooted hydrophyte with subaerial floating leaves). The latter four species have been sampled in smaller numbers (Supplementary Table S1) due to difficulties in locating/reaching them (*L. salicaria*, *G. uliginosum*, *N. alba*) and different morphology (*E. fluviatile*). All the plants listed above are common Eurasian wetland species, which are also widespread worldwide at the genus level (e.g., McNaughton, 1966; Mulligan et al., 1983; Theocharopoulos et al., 2006; Bryson and Carter, 2008; Trin et al., 2014).

2.2 Sampling

Mediterranean spring is a relatively wet season, with the highest growth rate for plants. Conversely, low precipitation and high temperatures enhance local aridity in summer, lowering the water level of the mire. This enhances plant water stress, strongly slowing their growth rate (Vilà and Sardans, 1999; Peichl et al., 2018). With the intention to highlight potential resulting seasonal differences, we sampled at both sites in summer 2014 (5th to 7th July) and spring 2015 (26th to 30th May).

We analysed a total of 452 samples (Supplementary Table S1); of these, the majority (229) were samples of fully developed leaves, collected from the apical, Sun exposed sections of each plant. Similarly, 161 samples were collected from the base of the main stem (except for *N. alba*). All leaf and lower stem samples come from different mature individuals of a species, sampled in close proximity, and complemented by a total of 47 soil samples collected at ca. 20 cm depth within each sampling station, from patches not directly exposed to sunlight to avoid potential ^2H-fractionation bias due to intense soil water evaporation. Additionally, 10 surface water samples were collected from swamp areas in proximity of the sampling stations at both sites.

All samples were collected during mid-daytime (ca 10:00 to 17:00), with mean air temperatures of 24°C–28°C (Nisí) and 28°C–29°C (TP) in summer, and 21°C–24°C (Nisí) and 26°C (TP) in

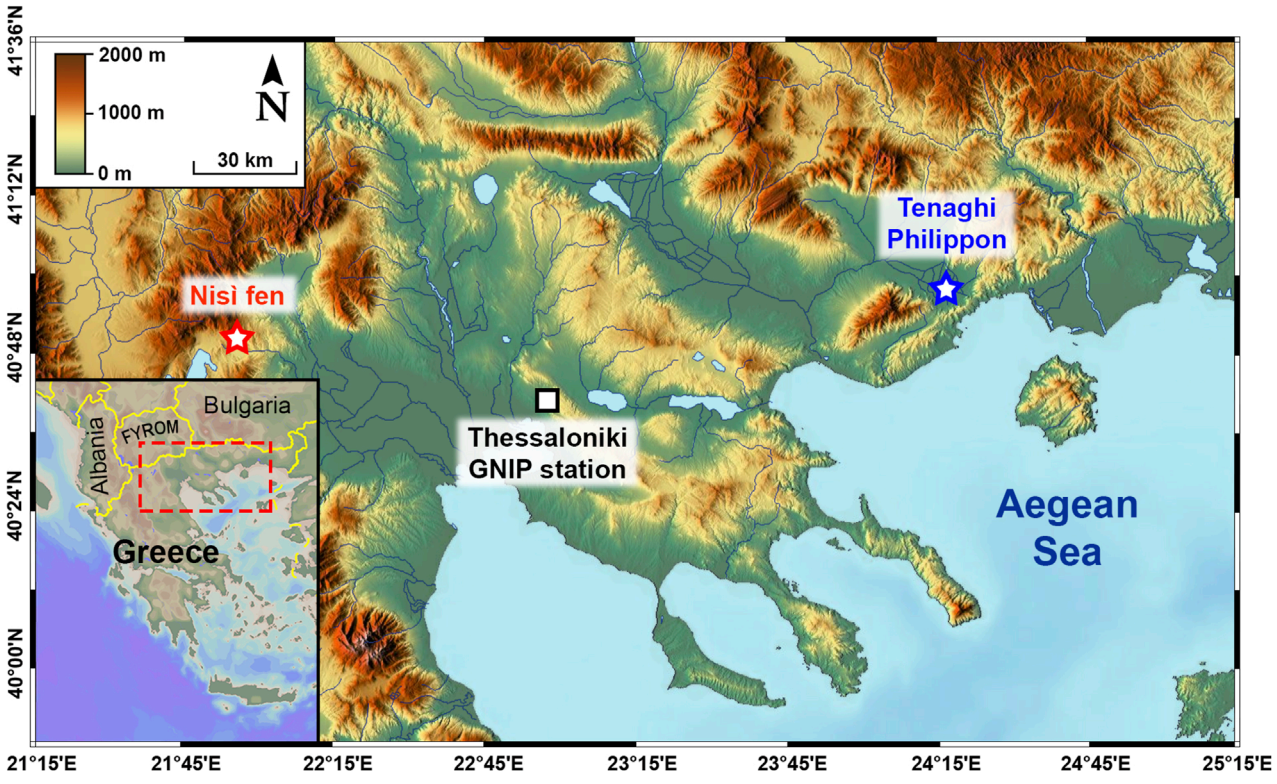

FIGURE 1
Map of northern Greece with the location of the two sampling sites and of the Thessaloniki GNIP station. Base map from Schlitzer, (2007); OpenStreetMap contributors, (2018).

spring. The selected leaves and the lower stem sections were severed with a clean metal knife. Additionally, we quickly and carefully de-veined eudicot leaves with a clean metal blade to avoid mixing the water contained in leaf cells with that present in the leaf vascular system. All samples (folded leaves, stem sections and subsurface soil) were then inserted into glass gastight vials (Labco Exetainer©), placed in a field refrigerator maintained at 5°C and subsequently frozen at −20°C in the laboratory. Surface water samples were collected in LDPE plastic bottles (60 mL), completely filled, tightly sealed, and kept refrigerated at max 5°C until analysis.

2.3 Water extraction and isotopic analysis

δ^2H values of the 10 surface water samples were obtained using a Los Gatos Research liquid water isotope analyser–cavity ringdown laser spectroscopy (LGR LWIA-24d) at the Senckenberg BiK-F laboratories, Frankfurt. Delta values are given as permil deviation from VSMOW (±1‰).

Leaf, stem, and soil water was extracted through cryogenic vacuum distillation and its isotopic composition was measured using a Thermo Electron high temperature conversion elemental analyser coupled to a Delta^{Plus}V mass spectrometer (TC/EA-MS) via a Conflo IV interface, at the Botanical Institute laboratories of the University of Basel, following the procedure described in Newberry et al. (2017). The hydrogen and oxygen isotopic compositions are expressed as permil deviation from VSMOW and the long-term external precision was found to be ±0.8‰ (standard deviation).

2.4 *n*-Alkane quantification and isotopic analysis

We obtained and measured *n*-alkanes in all 47 soil samples. Due to the high number of leaf and stem samples, we carefully selected a subset of 137 samples (105 leaf and 32 stem, ca. 3 leaf and 1-2 stem samples per each species per sampling station) from the original population to facilitate *n*-alkane analysis. The selection process ensured that each species was adequately represented and that the subset population reflected the water isotopic characteristics (δ^2H) of the original population (Table 3B).

The *n*-alkanes of leaf, stem and soil samples were extracted via accelerated solvent extraction, following the procedure described in Ardenghi et al. (2017), analysed via a ThermoScientific Trace GC Ultra–DSQII (GC-MS), and quantified using an external standard (Alk C_7-C_{40} – Supelco 49452-U, 1,000 ng/μL) at the Senckenberg BiK-F laboratories in Frankfurt a.M., Germany. The *n*-alkane δ^2H values of leaf and stem samples were determined using a ThermoScientific GC-Isolink II gas chromatograph coupled to a Delta^{Plus}V isotope ratio mass spectrometer via a ConFlo IV interface (GC-irMS), following the same procedure described in Ardenghi et al. (2019), at the physiological plant ecology laboratory at the Institute of Botany of the University of Basel, Switzerland. The

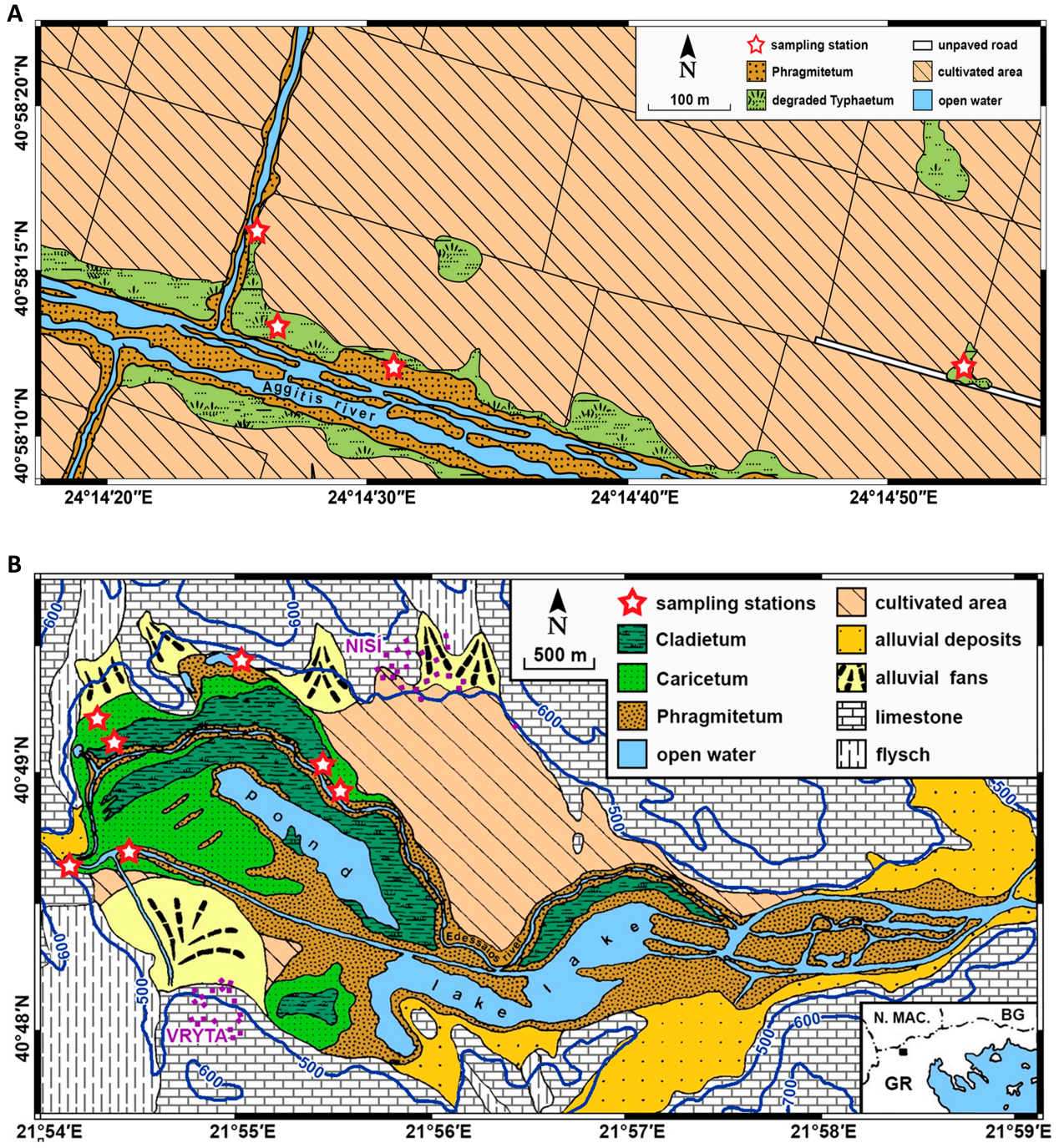

FIGURE 2
Stylised maps of main vegetation communities and surface geology of **(A)** the Tenaghi Philippon site, and **(B)** the Nisí fen site (modified from Christanis, 1994), including our sampling stations (created with ArcGIS pro; Esri, 2023).

overall analytical uncertainty (pooled sample size weighted standard deviation) was found to be ±1.7‰ (Polissar and D'Andrea, 2014). All *n*-alkane homologues (odd- and even-numbered) analysed for δ^2H with peak areas over 2 Vs were evaluated. However, as the linear response was tested only above 15 Vs, a correction for peak areas lower than 40 Vs was applied, based on a non-linear regression curve derived by an internal standard (Squalane; see Supplementary Material S1, Supplementary Figure S1).

The distribution of *n*-alkanes is summarised by two indices: the carbon preference index (CPI; Eq. 1; Marzi et al., 1993), and the average chain length index (ACL; Eq. 2; Poynter, 1989). Both indices are calculated on the $C_{14\text{-}37}$ homologue range.

$$CPI = \frac{\left(\sum_{i=n}^{m} C_{2i+1}\right) + \left(\sum_{i=n+1}^{m+1} C_{2i+1}\right)}{2\left(\sum_{i=n+1}^{m+1} C_{2i}\right)} \quad (1)$$

TABLE 1 Main topographical and environmental parameters of the two sampling sites.

	Nisí fen	Tenaghi Philippon basin
Coordinates	40°48′N 21°56′E	40°58′N 24°15′E
Elevation asl	475–480 m	43 m
Area	1,000 ha	5,500 ha
Mean summer temperature	23.0 °C	23.9 °C
Mean winter temperature	3.5 °C	5.5 °C
Average precipitation	725 mm/a	500 mm/a

$$ACL = \frac{\sum_i^m [C_{2i+1} \times (2i+1)]}{\left(\sum_i^m C_{2i+1}\right)} \quad (2)$$

To obtain an isotopic value comparable between samples with different homologue distribution, we calculated the hydrogen isotopic composition of the concentration weighted mean *n*-alkane (δ^2H_{CWMA}; Eq. 3; Newberry et al., 2015). Where *k* is the carbon number of the considered homologues, *n* the number of individual homologues recovered per sample (in the C_{15}–C_{37} range), and *total* indicates the sum of *n* homologues:

$$\delta^2H_{CWMA} = \sum_{k=n} \frac{\delta D_k \times Conc_k}{Conc_{total}} \quad (3)$$

In our data, we also detected a consistent pattern in the relative difference between the δ^2H of odd and even homologues. To express numerically this difference and allow its comparison between samples, we devised the "parity isotopic difference index" (PID, Eq. 4).

$$PID = \frac{\left[\sum_{i=n}^{m}(C_{2i+2}\text{-}C_{2i+1}) \Longleftrightarrow C_{2i+2} \wedge C_{2i+1} \neq \emptyset\right] + \left[\sum_{j=q}^{p}(C_{2j}\text{-}C_{2j+1}) \Longleftrightarrow C_{2j} \wedge C_{2j+1} \neq \emptyset\right]}{\sum_{k=s}^{r} C_k/C_k \Longleftrightarrow C_k \wedge C_{k+1} \neq \emptyset} \quad (4)$$

The formula indicates the average δ^2H difference between adjacent odd-even homologues (double headed arrow means "if, and only if," "C" is the δ^2H value of the respective homologue), and it is designed to buffer against missing data (Ø) and remove from the calculation any pair of non-adjacent homologues (to reduce the skewing influence due to potential drift in different areas of the analytical range).

Positive PID values indicate that odd homologues are generally more ^2H-depleted than even homologues, and *vice versa*; high absolute values indicate strong odd/even ^2H-difference and *vice versa*, while zero indicates no overall difference.

Isotopic ^2H-fractionation between the different hydrogen pools of surface water ($\delta^2H_{surfacew}$), soil water (δ^2H_{soilw}), lower stem water (δ^2H_{stw}), leaf water (δ^2H_{lw}) and *n*-alkanes (δ^2H_{stwax} for stems and δ^2H_{lwax} for leaves) was calculated according to Eq. 5 (Coplen, 2011); both δ and ε are then expressed as permil units (‰; Cohen et al., 2007).Where *a* and *b* represent the different hydrogen pools:

$$\varepsilon_{a-b} = \left[\frac{\delta^2H_a + 1}{\delta^2H_b + 1}\right] - 1 \quad (5)$$

Here we define $\varepsilon_{stw\text{-}lw}$ as the ^2H-fractionation between each species mean seasonal leaf water δ^2H and the respective mean lower stem water δ^2H. ^2H-fractionations between plant water and wax *n*-alkanes are indicated as $\varepsilon_{stw\text{-}stwax}$ (stem/stem), $\varepsilon_{stw\text{-}lwax}$ (stem/leaf) and $\varepsilon_{lw\text{-}lwax}$ (leaf/leaf).

3 Results

3.1 *n*-Alkanes

3.1.1 *n*-Alkane concentrations

The concentration of *n*-alkanes (*n*-$C_{14–37}$) in our plant samples (Supplementary Figure S2; Table 2) exhibited a wide range, spanning from 1.3 to 2,147.3 μg/g. In contrast, soil samples displayed relatively lower and less variable concentrations, ranging from 0.4 to 45.5 μg/g).

Concentrations were higher in eudicots/forbs and lower in monocots/graminoids. Leaves consistently showed approximately the same to ~80 times more *n*-alkanes than their corresponding lower stem samples (Table 2). This distinction between leaves and stems was notably pronounced among forbs in spring, while graminoids, such as *C. mariscus* and *S. lacustris,* exhibited less overall leaf/stem differentiation. Our data revealed no consistent difference in *n*-alkane concentrations between spring and summer at either site. Nevertheless, the leaves of four species (*S. Palustris, C. longus, S. lacustris* in Nisí, and *P. australis* in TP) exhibited a spring-to-summer increase in mean concentration surpassing their respective standard deviation (Table 2). Similarly, while no distinct difference emerged between samples of the same species from Nisí and TP (only four species in common; Supplementary Table S1), leaves of *C. longus* and *P. australis* showed higher *n*-alkane concentration in TP, albeit often close to the respective standard deviation values; Table 2).

3.1.2 *n*-Alkane distribution

The carbon preference index (CPI) exhibited a wide range across samples: from 0.4 to 86.2 in leaves (with a mean of specific averages at 16.1 ± 7.6), 1.8 to 54.4 in lower stems (mean of specific averages at 14.4 ± 7.1), and 0.9 to 10.4 in soil samples (mean of specific averages at 5.2 ± 1.7). Overall, CPI displayed considerable inter- and intra-specific variability, with all samples recording values well above 1,

TABLE 2 *n*-alkanes absolute concentrations (μg/g), with relative standard deviation (σ), carbon preference index (CPI) and average chain length (ACL) for all leaf, lower stem, and soil samples (*n* = 187) analysed in this study.

			Nisí fen										Tenaghi Philippon									
			Spring					Summer					Spring					Summer				
			μg/g	σ	CPI	ACL	n	μg/g	σ	CPI	ACL	n	μg/g	σ	CPI	ACL	n	μg/g	σ	CPI	ACL	n
Leaf	C_3 forbs	*C. palustris*	335	206	58.4	29.2	3	226	38	14.7	29.6	3										
		G. uliginosum						89	23	19.1	28.9	3										
		L. salicaria						365	326	8.7	29.9	3										
		M. aquatica	1955	167	7.7	31.0	3	621	281	8.8	31.7	4										
		S. palustris	123	60	10.5	29.0	3	1191	473	8.7	31.2	3										
	C_3graminoids	Group average	804	157	25.5	29.7	3	498	287	12.0	30.3	5										
		without GU and LS	804	157	25.5	29.7	3	679	318	10.7	30.8	3										
		C. riparia	155	118	26.0	29.5	6	195	104	18.3	28.6	7										
		C. mariscus	485	239	15.5	27.8	6	289	45	6.9	27.7	3										
		P. australis	32	13	17.6	28.3	6	63	38	4.5	28.1	6	63	24	27.2	28.5	3	168	70	20.6	28.1	3
		S. lacustris	27	10	5.3	27.2	3	151	53	52.5	30.7	3	31	18	6.9	27.9	3					
		T. angustifolia	128	75	13.2	28.3	6	199	109	2.8	28.3	3	114	37	13.9	28.6	3					
		Group average	165	124	15.5	28.2	5	179	76	17.0	28.7	5	69	27	16.0	28.3	3					
		C. longus (C_4)	24	1	23.2	29.6	3	43	18	2.8	29.2	8	69	6	26.5	31.2	3					
		E. fluviatile	70	13	11.6	25.8	3	10.2[a]		6.6[a]	26.2[a]	1										
		N. alba						12	6	3.6	28.1	3										

(Continued on the following page)

10.3389/feart.2024.1359157

TABLE 2 (*Continued*) *n*-alkanes absolute concentrations (μg/g), with relative standard deviation (σ), carbon preference index (CPI) and average chain length (ACL) for all leaf, lower stem, and soil samples (*n* = 187) analysed in this study.

			Nisí fen										Tenaghi Philippon									
			Spring					Summer					Spring					Summer				
			μg/g	σ	CPI	ACL	n	μg/g	σ	CPI	ACL	n	μg/g	σ	CPI	ACL	n	μg/g	σ	CPI	ACL	n
Lower Stem	C_3 forbs	*C. palustris*	4		5.1	27.6	1	57		26.5	29.6	1										
		L. salicaria						18		4.0	28.8	1										
		M. aquatica	25		12.6	30.5	1															
		S. palustris	13		8.4	28.6	1	75		7.6	30.5	1										
	C_3graminoids	Group average	14		8.7	28.9	3	50		12.7	29.6	3										
		C. riparia	13	6	11.4	23.1	2	195	261	24.6	27.0	2										
		C. mariscus	380	360	34.7	27.6	2	215		22.1	28.2	1										
		P. australis	15	5	13.3	28.5	2	8	10	7.0	27.4	2	4		18.0	28.7	1	6		5.5	27.6	1
		S. lacustris	64		15.0	28.5	1	15			31.2	1	69		9.4	28.4	1					
		T. angustifolia	9	2	10.0	27.7	2	7	2	4.7	27.5	2	162		27.3	23.9	1					
		Group average	96	180	16.9	27.1	5	88	151	14.6	28.3	5	78		18.2	27.0	3					
		C. longus (C_4)	3		9.0	22.1	1	6	5	7.4	27.5	3	80		29.6	31.7	1					
		E. fluviatile	33		18.9	25.3	1															
Soil			20	9	6.0	28.1	6	21	11	7.0	28.7	20	15	3	3.0	27.3	12	13	8	4.8	28.1	9

[a]Values referring to a "whole" *E. fluviatile* fertile shoot sample.

10.3389/feart.2024.1359157

except for three *C. longus* leaf samples, characterised by low *n*-alkane concentrations (Table 2). This suggests a prevalent odd-over-even predominance, notably stronger in plant samples (with a mean of 15.2 ± 7.3) than in soil samples. The sole discernible pattern was seasonal, with CPI generally decreasing from spring to summer, especially in graminoids (Supplementary Table S3) in both leaf and lower stem samples.

The average chain length index (ACL) exhibited a diverse range across samples: from 25.5 to 32.0 in leaves (with a mean of specific averages at 29.0 ± 0.5), 21.4 to 31.7 in stems (mean of specific averages at 27.7 ± 0.6), and 26.4 to 29.4 in soil samples (mean of specific averages at 28.0 ± 0.7). Most samples fell within the typical ACL range for terrestrial plants (27–31), including the floating hydrophyte *N. alba*. The exception was *E. fluviatile*, the only pteridophyte (i.e., seedless/flowerless vascular plants, mostly ferns) analysed in this study, with an ACL range of 25–26. Eudicots/forbs and leaves showed ACL higher than, respectively, monocots/graminoids and stems (Supplementary Table S3), as well as soil samples (ca. 27–29). ACL also showed a general increase from spring to summer in eudicot/forb leaves (average increase of 0.4–2.2), although stability was observed in monocot/graminoid leaves. Most stem samples showed an average increase of 0.6–5.8 during this seasonal transition.

3.1.3 *n*-Alkane hydrogen stable isotopic composition

Plant wax *n*-alkane δ^2H values in the C_{20-35} range exhibited a broad spectrum, ranging from −281‰ to −48‰ (mean ≈ −180‰, σ ≈ 41‰; detailed descriptive statistics for each homologue are reported in Supplementary Table S4). Notably, even chain lengths displayed generally less depleted values (mean ≈ −140‰) compared to odd chain lengths (mean ≈ −171‰; Figure 3). For both odd and even homologues, the most depleted values were observed in the C_{27-31} range (odd ≈ −179‰, even ≈ −147‰), while progressively less depleted values characterised shorter (odd ≈ −171‰, even ≈ −154‰) and longer (odd ≈ −176‰, even ≈ −129‰) homologues.

The δ^2H weighted mean (δ^2H_{CWMA}) strongly reflected the values of C_{27}-C_{29} and C_{31}, the three most abundant homologues in all leaf samples and most lower stem samples (Supplementary Table S4). In leaf samples, δ^2H_{CWMA} ranged from −273‰ to −115‰ (average −198‰ ± 28‰), while in stem samples, it ranged from −253‰ to −152‰ (average −196‰ ± 27‰). Among leaf samples, species with the least depleted δ^2H values were *G. uliginosum* among forbs, *C. longus* among graminoids, *E. fluviatile,* and *N. alba,* while *M. aquatica* and *C. mariscus* exhibited the most depleted values. Lower stem samples displayed higher interspecific variability.

Summer δ^2H values of concentration-weighted mean *n*-alkanes from leaves (CWMA δ^2H_{lwax}) were generally less depleted than spring values (Supplementary Table S3; Figure 4), with exception noted for *S. lacustris* and *E. fluviatile* (likely influenced by sampling bias; see Section 4.2.3), as well as *S. palustris* and *C. riparia*. In Nisí, focusing on C_3 species, graminoids exhibited the most depleted δ^2H_{lwax} (−214‰, −215‰), while generally less depleted values (Supplementary Table S3) characterised forbs (−205‰, −183‰) and *E. fluviatile* (−171‰).

3.2 Hydrogen stable isotopic composition of water

3.2.1 Surface and soil water ^2H composition

Surface and soil water δ^2H values (Figure 5; Supplementary Table S2) varied between −72‰ and +37‰. Across both sites and seasons, the δ^2H values for surface and soil water were well clustered around their means, with a maximum standard deviation of 1.8‰. Notably, surface water maintained a consistent mean δ^2H value (ca −54‰) in both seasons at both sites. In contrast, soil water δ^2H values consistently trended lower in Nisí compared to TP, demonstrating an increase from spring (−49.1‰ TP; −60.2‰ Nisí) to summer (−46.5‰ TP; −49.9‰ Nisí; Supplementary Table S2). Both surface water and soil water showed more ^2H-depleted values compared to water from leaves and lower stems.

3.2.2 Lower stem water and leaf water δ^2H values

Leaf water δ^2H values for ranged from 37‰ to −41‰, with two outliers at −71‰ (mean ≈ −8‰, median ≈ −8‰, σ ≈ 14‰). In contrast, lower stem water δ^2H values varied between −18‰ and −65‰ (mean ≈ −49‰, median ≈ −49‰, σ ≈ 10‰).

Seasonal, species-specific mean δ^2H values for lower stem water ranged from −62‰ to −24‰, while leaf water values ranged from −25‰ to +29‰. Except for those of *M. aquatica*, *S. palustris*, and *S. lacustris*, spring values typically exhibit a greater ^2H-depletion compared to summer values (approximately 5‰–15‰). However, the variability closely aligned with the standard deviation for each species, as outlined in Table 3B and Figure 5. Similarly, for both lower stem and leaf water, forbs displayed higher δ^2H values than graminoids (ca 5‰–10‰ on average) and TP showed higher values than Nisí (Table 3B; Supplementary Table S3). Stem to leaf water ^2H-fractionation ($\varepsilon_{stw\text{-}lw}$) ranged between +13‰ and +59‰ (Table 3B).

4 Discussion

4.1 Variability of *n*-alkane concentration/distribution in plants and soil

4.1.1 Variability between plant forms and between leaves and stems

Leaf samples show consistently higher *n*-alkane concentrations than stem samples (up to 80 times and ca. 15 times on average; 3.1.1, Table 2). This can be attributed to the necessity for a thicker cuticle to mitigate desiccation in the upper organs, more exposed to sunlight (i.e., leaves and flowers; Gamarra and Kahmen, 2015; Speckert et al., 2023). More in detail, while forbs show on average higher leaf *n*-alkane concentrations than graminoids, they also show greater difference between leaves and stems (40 times on average) than graminoids (7 times on average). This is common (e.g., He et al., 2020; Corcoran et al., 2022) and likely due to morphological differences between these two groups.

The CPI (Table 2) shows no consistent differences between species nor between leaves and stems, with several species (e.g., *P. australis, C. palustris*) exhibiting contrasting leaf-to-stem CPI ratio values in different sampling instances. The CPI values decrease

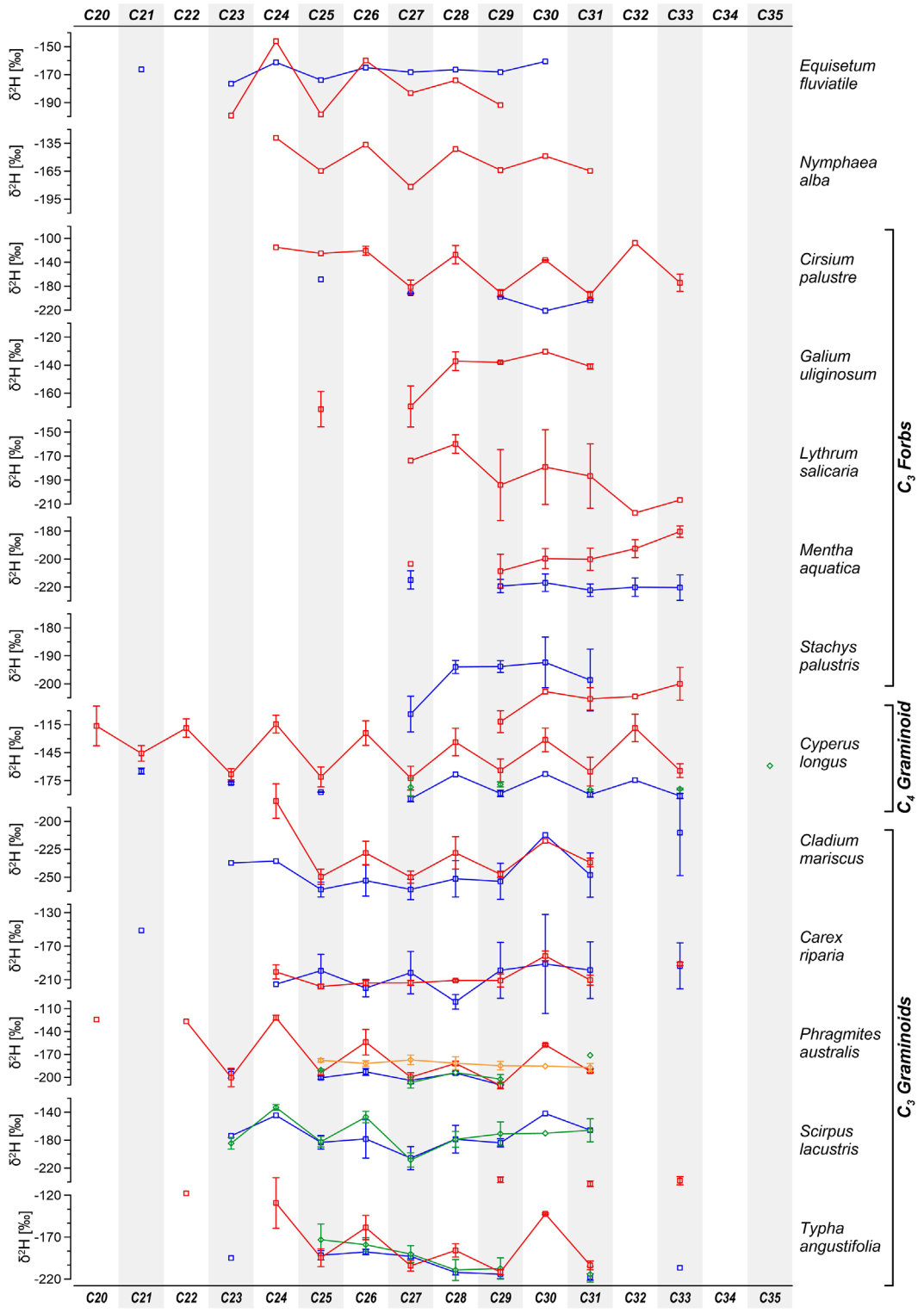

FIGURE 3
Average δ^2H values of individual *n*-alkane homologues from leaf samples divided by species, season and sites: blue (spring/Nisí), red (summer/Nisí), green (spring/TP), orange (summer/TP). Error bars indicate the standard error of the mean.

from leaf/stem samples to soil, likely due to preferential degradation of longer homologues (Yan et al., 2021) and the production of microbial derived shorter/even homologues (Thomas et al., 2021; Corcoran et al., 2022 and refs therein), making it impossible to use CPI as a proxy to trace specific plant sources in sediments (Chen et al., 2022).

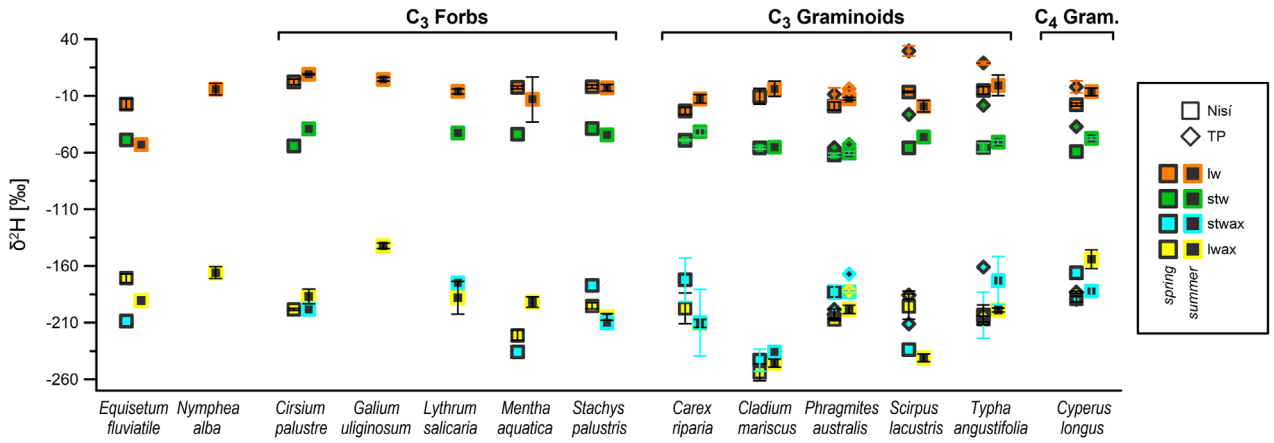

FIGURE 4
Mean δ^2H values of leaf and lower stem water (lw; stw) and leaf and lower stem wax *n*-alkanes (lwax; stwax), by species, season and site. Vertical bars indicate SEM.

In terms of ACL, leaves show similar, although generally higher values then the corresponding stem samples (Table 2). Relative to leaves, stem samples often display a broader distribution of odd chain lengths centred around the same C_{max} (Supplementary Figure S2), along with analogous but generally lower ACL values, with a few exceptions (e.g., *C. riparia* in Nisí in spring; Table 2). These observations align with previously reported differences between leaves and roots in C_4 grasses such as *Enneapogon avenaceus* and *Astrebla pectinata* (Kuhn et al., 2010), but are in contrast with the findings of He et al. (2020) for similar Poaceae and Cyperaceae emergent species, reporting much lower ACL values in roots relative to leaves. The similarity in ACL and the higher concentrations of *n*-alkanes in leaves compared to stems indicate that, as observed in alpine and temperate grassland species (Gamarra and Kahmen, 2015), also in these fen environments the distinctive signal deposited in sediments is predominantly characterized by the chain length distribution of the leaves (and not the stems) of helophytic plants.

In terms of plant forms, ACL values in our data generally differ between forbs and graminoids. Graminoids leaves exhibit lower ACL (27–29) than forbs leaves (29–32), with the exception of the C_4 graminoid *C. longus* (29–31), as highlighted by the PCA in Figure 6; stem samples show an analogous pattern. Very slight, although opposite, differences between forbs and graminoids ACL have been detected before on plants from a similar fen environment on the Chinese Loess Plateau (Liu et al., 2018). Overall, graminoids show higher values on the Chinese Loess Plateau (~30.0) than in Nisí and TP (~28.6), while forbs have a similar/lower ACL range than graminoids (Supplementary Table S3). On one hand, this opposite behaviour of ACL could be a response to the differences between the climates of the Chinese Loess Plateau (Köppen BS) and of the Mediterranean borderlands. In fact, even if both are characterised by seasonal aridity, the timing is different between these two regions: on the Chinese Loess Plateau winter (and not summer) is the most arid season (Kong et al., 2018). Alternatively, the different behaviour of ACL in our study could simply be the result of different species associations (Diefendorf et al., 2021).

Also, the other two plant forms present in our data show ACL values lower than forbs/eudicots. The floating hydrophyte *N. alba* shows an ACL (~29) more characteristic of emerged helophytes (probably indicating the subaerial condition of its leaf blades; Yu et al., 2021). Interestingly, the only pteridophyta (*E. fluviatile*) shows an ACL (25–26, the lowest in our results) closer to submerged hydrophytes than to terrestrial plants (Figure 6; Yu et al., 2021).

In our soil samples, ACL is relatively stable (27.3–28.7; Table 2) and mean values tend to be similar to mean ACL values of monocots/graminoids (leaves and stems) in both locations and seasons, likely reflecting a major contribution of this plant group to sediment/peat deposition (Liu et al., 2018), as also highlighted in the PCA (Figure 6).

We are aware that caution must be applied to the interpretation of ACL environmental significance, as (1) it has already been shown that relative humidity gradients can have opposite effects on the ACL of different species (Hoffmann et al., 2013; Chen et al., 2022) and (2) plant contributions to sediments in any environment is subject to multiple taphonomic variables (e.g., Corcoran et al., 2022 and refs therein). However, our results indicate ACL as a potential tool to differentiate between plant form (forbs vs. graminoids) relative contribution in this particular environment. Based on our data, the *n*-alkane signal stored in the sediments of this fen environment with this type of helophytic plant community seems to be mostly representative of local graminoids, and particularly of their leaves.

4.1.2 Seasonality

Our samples show no consistent change in *n*-alkane concentration between seasons, at both sites (Table 2). While *S. palustris*, *C. longus*, and *S. lacustris* leaves show clear increases from spring to summer, the opposite is true for *M. aquatica*, *C. mariscus*, and *E. fluviatile*, while values for all the other species remain within a standard deviation and thus substantially unvaried. Concentrations are expected to positively correlate

TABLE 3 Hydrogen stable isotopic composition of (A) soil water and surface water, and (B) internal water and *n*-alkanes of lower stem and leaf samples, divided by species and season.

		Spring			Summer		
		δ^2H	σ	n	δ^2H	σ	n
A							
Nisí fen	Soil water	−60	5	6	−50	3	20
	Surface water	−54	1	6	−56	0	1
TP	Soil water	−49	8	12	−47	5	9
	Surface water	−54	0.5	2	−54	0	1

			Spring												Summer											
			Water						*n*-alkanes (CMWA)						Water						*n*-alkanes (CMWA)					
			Lower stem			Leaf			Lower stem			Leaf			Lower stem			Leaf			Lower stem			Leaf		
			δ^2H	σ	n	δ^2H	σ	n	δ^2H	σ	n	δ^2H	σ	n	δ^2H	σ	n	δ^2H	σ	n	δ^2H	σ	n	δ^2H	σ	n
B																										
Nisí fen	C_3forbs	*C. palustris*	−53 (−54)		5(1)	2 (2)	4(4)	5(3)				−198	1	3	−39(−39)		3(1)	9(9)	1(1)	5(3)	−198		1	−187	9	3
		G. uliginosum																5(5)	2(3)	5 (3)				−142	3	3
		L. salicaria													−43 (−43)		1(1)	−6(−6)	4(4)	3(3)	−175		1	−188	20	3
		M. aquatica	−43(−44)		5(1)	−2(−3)	2(3)	5(3)	−236		1	−221	6	3				−25(−13)	43(40)	5(4)				−192	8	4
		S. palustris	−38(−39)		5(1)	−2(−2)	2(3)	5(3)	−177		1	−195	4	3	−44(−44)		5(1)	−4(−3)	4(5)	5(3)	−210		1	−205	4	3
		Group average	−45(−46)		3(3)	−1(−1)	2(3)	3(3)	−206	41	2	−205	14	3	−44(−44)	3(3)	3(3)	−4(−2)	13(9)	5(5)	−194	18	3	−183	24	5
		GU and LS	−45(−46)		3(3)	−1(−1)	2(3)	3(3)	−206	41	2	−205	14	3				−7(−2)	17(11)	5(5)						
	C_3graminoid	*C. riparia*	−49(−49)	3(1)	10(2)	−23(−23)	7(7)	10(6)	−172	19	2	−197	30	6	−42(−42)	4(4)	10(2)	−13(−13)	8(10)	20(7)	−210	29	2	−211	9	7
		C. mariscus	−56(−56)	2(2)	10(2)	−15(−10)	17(17)	10(6)	−243	10	2	−254	17	6	−54(−55)		5(1)	0(−4)	12(12)	10(3)	−236		1	−246	5	3
		P. australis	−62(−62)	2(2)	10(2)	−19(−19)	7(9)	10(6)	−204	6	2	−207	2	6	−60(−60)	2(2)	11(2)	−12(−13)	4(3)	20(6)	−183	1	2	−198	8	6
		S. lacustris	−55(−56)		5(1)	−6(−7)	1(1)	5(3)	−234		1	−196	16	3	−34(−46)		5(1)	−21(−19)	7(9)	10(3)				−241	5	3
		T. angustifolia	−55(−55)	4(5)	10(2)	−5(−5)	6(8)	10(6)	−203	20	2	−207	6	6	−52(−51)	3(3)	11(2)	−4(−1)	15(16)	16(3)	−173	21	2	−199	2	3
		Group average	−55(−56)	5(5)	5(5)	−14(−13)	8(8)	5(5)	−211	12	5	−212	15	5	−48(−51)	10(7)	5(5)	−10(−10)	8(7)	5(5)	−200	28	4	−219	23	5
		C. longus(C_4)	−60(−59)		5(1)	−20(−18)	7(2)	5(3)	−166		1	−189	4	3	−48(−47)	4(2)	15(3)	−6(−6)	9(10)	25(8)	−182	6	3	−154	22	8
		E. fluviatile	−49(−49)		5(1)	−19(−17)	6(8)	5(3)	−209		1	−171	5	3	−53(−53)		5(1)				−190 *		1			
		N. alba																−2(−4)	7(9)	5(3)				−166	7	3

(Continued on the following page)

10.3389/feart.2024.1359157

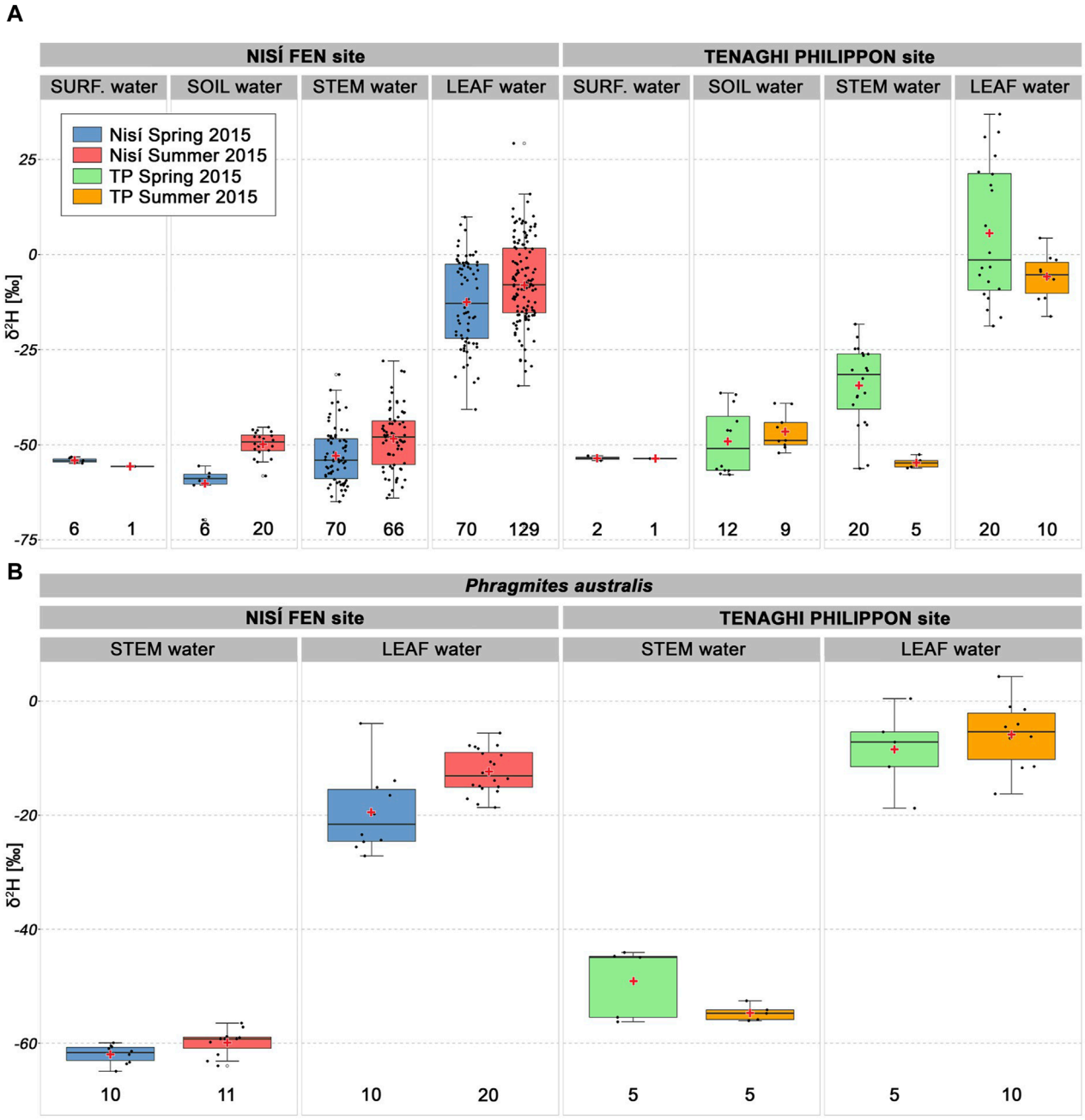

FIGURE 5
(A) Boxplots comparing δ^2H values of surface water, soil water, lower stem water and leaf water (n = 452), divided by site and season. Red crosses mark simple means, black dots individual values, empty dots outliers, black line the median; bottom numbers indicate sample size. The subset for *P. australis* **(B)** shows how the negative spring to summer δ^2H shift for plant water at the TP site, apparent in **(A)**, is due to missing summer data-points for the other collected species.

to the summer temperature increase, to enhance the cuticular transpiration barrier, as shown, for example, in *Juniperus monosperma* leaves, (Diefendorf et al., 2021; Shi et al., 2021 and refs therein). The reason behind this inconsistency is unclear, but it likely results from the effect of other factors controlling *n*-alkane production and preservation, such as, for example, leaf abrasion, aridity, and variability in the leaf sampling procedure (Eglinton and Eglinton, 2008).

Similarly, ACL values do not show a clear seasonal pattern. Forbs such as *C. palustris, M. aquatica, S. palustris,* as well as *S. lacustris* and *E. fluviatile* show increasing ACL values from spring to summer, but all other species show no clear seasonal change. While seasonal ACL increases have been detected before (e.g., from April to September in *Salix viminalis* leaves, Newberry et al., 2015, in other eudicot/monocot species, Cui et al., 2008, and even in a 15 years study of a subalpine meadow, Shi et al., 2021), Diefendorf et al.

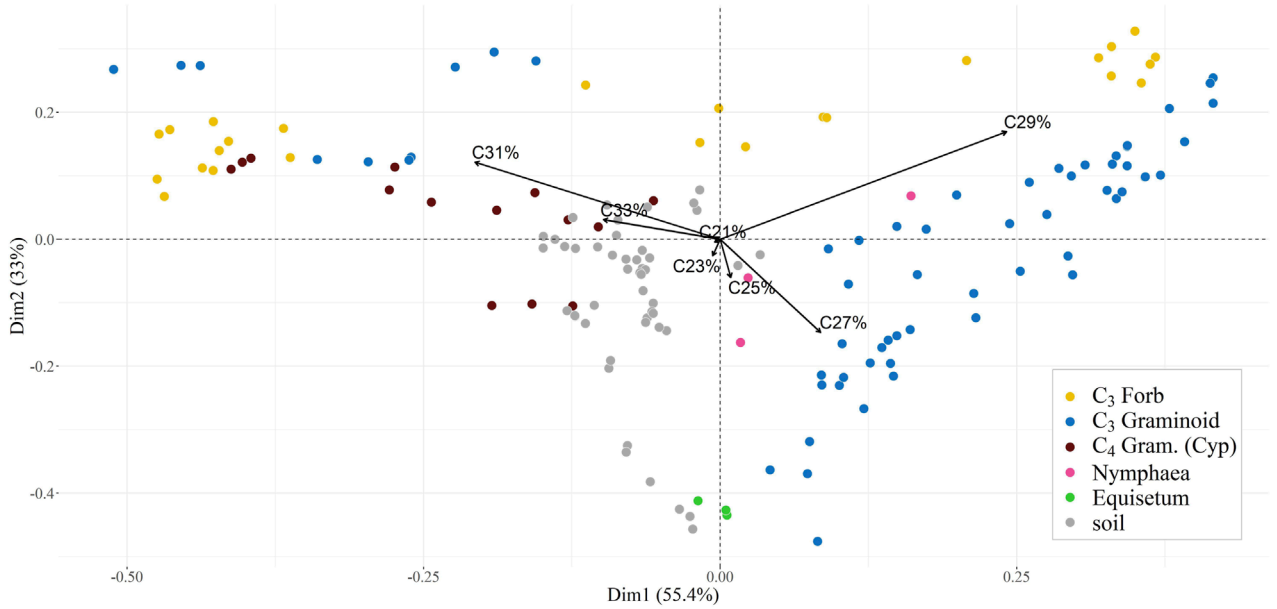

FIGURE 6
Principal component analysis scores for proportional abundances (0-1) of C_{21-33} *n*-alkane concentrations (odd homologues only), for soil samples and leaf samples, divided by growth form and photosynthetic pathway. *Nymphaea alba* (being a floating hydrophyte) and *Equisetum fluviatile* (the only pteridophyte) have been assigned to two separate classes. The distribution of the sample groups describes more in detail what already suggested by ACL values. C_3 forbs, mainly characterised by C_{31}, C_{33} and C_{29} predominance, are separated by the majority of C_3 graminoids, characterised by a strong C_{27} and C_{29} components (except for a few *S. lacustris* and *C. riparia* samples), as is the aquatic *N. alba* (probably reflecting the subaerial condition of its leaves). The C_4 graminoid *C. longus* plots between these two groups, while the fern *E. fluviatile* constitutes a separate cluster down the C_{23} and C_{25} directions. Soil samples clustering between C_3 and C_4 graminoids, (with several points in the C_{23} direction), seems to indicate an origin strongly controlled by these two groups. Produced with the R statistical software, using the FactoMiner package (Lê et al., 2008).

(2021) found ACL to be unrelated to temperature increases and to be instead relatively constant within a species. Based on our data, neither *n*-alkane concentration nor ACL do appear to provide valuable information on seasonality in these type of fen vegetational communities.

In contrast, CPI shows a consistent seasonal decrease from spring to summer. The decrease in CPI seems generally related to an increase of even homologues, while odd homologues concentrations appear relatively stable (Supplementary Figure S2). An analogous CPI seasonal pattern has been detected in maple leaves (Chikaraishi and Naraoka, 2006) and other eudicot/monocot species (Cui et al., 2008) and linked to leaf senescence. However, as none of our leaves/stems showed signs of fading when collected in July, this is an unlikely explanation for the seasonal CPI shift in our samples. Instead, the CPI increase could be related to the enhanced summer aridity. Drought conditions have been shown to speed up lipid metabolism while affecting enzymatic chain elongation, leading to an increased production of mid-short *n*-alkanes homologues and their relative degradation by-products, including even homologues (Post-Beittenmiller, 1996; Shepherd and Griffiths, 2006; Srivastava and Wiesenberg, 2018; Speckert et al., 2023).

In general, our data indicate that CPI values in plant samples differ between the growing (higher values) and the dry (lower values) seasons. However, due to preferential degradation and microbial activity (Thomas et al., 2021; Corcoran et al., 2022 and refs therein; see Section 4.1.1), soil/sediment CPI is likely an unreliable proxy for tracing seasonality in sediments, at least in this kind of Mediterranean fen environments.

4.2 Water ^{2}H signal from source to leaf water: precipitation and evapotranspiration

4.2.1 Mean annual precipitation as plant source water pool

Surface water and soil water at a depth of 20–30 cm exhibited very similar hydrogen isotopic values (Figure 5), pointing to a clear link between the two water pools. δ^2H values for surface and soil water show very similar ranges at both sites in each season (except for 3 unusually high values in TP spring soil water). This reinforces the hypothesis that the Nisí site can be considered as an analogue for the ancient TP site in terms of δ^2H of source water based on the opinion of researchers that have described the environmental, climatic, and geological characteristics of both sites (e.g., Christanis, 1994; Kalaitzidis, 2007; see Table 1) as well as on the data of spring/source water δ^2H reported here and throughout Greece (Dotsika et al., 2010).

The sole contemporary dataset for annual precipitation δ^2H (δ^2H_p) in northern Greece is derived from the Thessaloniki GNIP station, covering a period of 2.5 years from 2001 to 2003). The station is situated approximately 105 km W-SW of the Tenaghi Philippon peatland and 90 km E-SE of Nisí fen (IAEA/WMO, 2017; Figure 1).

TABLE 3 (*Continued*) Hydrogen stable isotopic composition of (A) soil water and surface water, and (B) internal water and *n*-alkanes of lower stem and leaf samples, divided by species and season.

		Spring										Summer									
		Water			*n*-alkanes (CMWA)							Water			*n*-alkanes (CMWA)						
		Lower stem			Leaf			Lower stem			Leaf	Lower stem			Leaf	Lower stem			Leaf		
		δ^2H	σ	n	δ^2H	σ	n	δ^2H	σ	n	δ^2H	σ	n	δ^2H	σ	n	δ^2H	σ	n	δ^2H	σ	n
TP		−49(−55)		5(1)	−8(−8)	7(10)	5(3)	−198		1	−203	6	3	−55(−53)		5(1)	−6(−4)	6(8)	10(3)	−167		1	−182	6	3
	P. australis																								
	S. lacustris	−28(−27)		5(1)	29(30)	6(8)	5(3)	−211		1	−186	5	3												
	T. angustifolia	−24(−18)		5(1)	5(19)	19(2)	5(3)	−161		1	−203	12	3												
	Group average	−34(−33)		3(3)		19(20)		−190		3	−197	7	3												
	C. longus(C_4)	−36(−37)		5(1)	−4(−2)	7(9)	5(3)	−189		1	−183	1	3												
C_3 gram.																									

Mean values for all the samples that underwent cryogenic vacuum distillation are compared to the means of the sample subset that underwent n-alkane extraction and isotopic analysis (reported between parentheses). All δ^2H and σ values are reported in permil (‰).

The δ^2H_p values range from −99‰ to −3‰ (with an annual precipitation weighted average of −48‰) and show a distinct seasonal pattern. The most negative values characterise the abundant precipitation during the wet winter-spring period reflecting a weighted mean of approximately −52‰. Conversely, the least negative are observed during the dry Mediterranean summer, hovering around −31‰. As a result, surface and soil water δ^2H at the end of spring serve as a reliable approximation of the δ^2H_p annual weighted mean (ca. −48‰).

Our data affirms this pattern, as soil (and surface) water consistently exhibit δ^2H values similar to this annual mean not only in spring (−49.1‰ in TP; −60.2‰ in Nisí), but also in summer (−46.5‰ in TP; −49.9‰ in Nisí). This alignment is likely attributed to the elevated amounts of winter-spring precipitation and, most probably, to the smearing effect of the karstic aquifer feeding the mire(s) (Kalaitzidis, 2007; Dotsika et al., 2010). Remarkably, the OIPC provides comparable annual δ^2H values for precipitation (−51‰ ± 2‰ in Nisí; −48‰ ± 1‰ in TP); similarly, local sampling in NW (−60.4‰ ± 0.8‰) and NE (−50.6‰ ± 0.7‰) Greece, where Nisí fen and TP are located, respectively, supports similar values for spring water (Dotsika et al., 2010). This suggests that these helophytic plant communities in these Mediterranean regions do indeed utilise water that faithfully represents local annual δ^2H_p values.

4.2.2 Soil water to lower stem water

Most species showed less depleted stem water δ^2H (δ^2H_{stw}) values in the summer, and, within the same species, δ^2H_{stw} values were less depleted in TP than in Nisí (Table 3B). The ^2H-fractionation between the soil water and the lower stem water ($\varepsilon_{soilw\text{-}stw}$) of each species (Table 4) was 1) consistently positive (except for *P. australis*), 2) often within the respective standard deviations, and 3) lacking a clear seasonal pattern. Additionally, as ^2H-fractionation during water absorption in roots is considered unlikely (Ehleringer and Dawson, 1992; White et al., 1994; Jacob et al., 2021), the tendency to less depleted δ^2H_{stw} values appears to reflect an occasional initial minor evapotranspiration effect occurring at the crown root and/or at the base of the stem (Eensalu et al., 2023). This difference is more pronounced for forbs (δ^2H_{stw} up to approximately 22‰ less depleted than δ^2H_{soilw}) than for graminids (generally in the 0‰–5‰ range) and mirrors the $\delta^{18}O$ differences between the soil and stem water of two grasses (*Dactylis glomerata, Lolium perenne*) and a forb (*Trifolium pratense*; Barnard et al., 2006). We speculate that the overall low/absent enrichment of stem water relative to soil water in monocots/graminoids might be attributed to a protective outer sheath present at the base of most grasses (which was removed during sampling; Barnard et al., 2006). The occasional negative difference between the δ^2H_{stw} and the δ^2H_{soilw} values for *P. australis* (down to ca. −10‰ in summer), could be explained by its greater rooting depth (Burdick et al., 2001; Moore et al., 2012; Huang et al., 2018; Zhao et al., 2018; Huang and Meyers, 2019), a phenomenon already documented for some species growing in arid environments (Feakins and Sessions, 2010; Corcoran et al., 2022).

Overall, the data indicates an absence of evaporative enrichment between soil and stem water or at the very least, a very limited occurrence of it. Despite specific variations in rooting depth, leading to a decoupling between δ^2H_{stw} and δ^2H_{soilw}, when considering the

TABLE 4 Values of ^{2}H-fractionation between soil water, plant internal water, and plant *n*-alkanes (CMWA; see Table 3B).

			Spring														Summer													
			$\varepsilon_{soilw\text{-}stw}$			$\varepsilon_{stw\text{-}lw}$			$\varepsilon_{lw\text{-}lwax}$			$\varepsilon_{lw\text{-}stwax}$			$\varepsilon_{stw\text{-}stwax}$			$\varepsilon_{soilw\text{-}stw}$			$\varepsilon_{stw\text{-}lw}$			$\varepsilon_{lw\text{-}lwax}$			$\varepsilon_{lw\text{-}stwax}$			$\varepsilon_{stw\text{-}stwax}$		
			Mean	Sem	n	Mean	Sem	n	Mean	Sem	n	Mean	Sem	n	Mean	Sem	n	Mean	Sem	n	Mean	Sem	n	Mean	Sem	n	Mean	Sem	n	Mean	Sem	n
Nisí fen	C_3 forbs	*C. palustris*	6	2	1	60	2	3	−188	2	3							12	1	1	50	1	3	−180	7	3	−192	1	1	−157	1	1
		G. uliginosum																					−135	3	3						
		L. salicaria															7	1	1	38	2	3	−181	15	3	−168	1	1	−133	1	1
		M. aquatica	18	2	1	43	1	3	−211	4	3	−226	1	1	−193	1	1							−185	5	4						
		S. palustris	23	2	1	38	2	3	−185	3	3	−167	1	1	−131	1	1	6	1	1	43	3	3	−199	3	3	−204	1	1	−170	1	1
	C_3graminoids	Group average	16	5	3	47	6	3	−195	8	3	−196	30	2	−162	31	2	8	2	3	44	3	3	−176	11	5	−188	10	3	−153	11	3
		C. riparia	12	2	2	27	3	6	−187	14	6	−162	19	2	−126	19	2	9	3	2	30	5	7	−204	4	7	−210	29	2	−169	29	2
		C. mariscus	5	2	2	48	7	6	−244	8	6	−234	10	2	−201	10	2	−6	1	1	54	7	3	−239	4	3	−229	1	1	−197	1	1
		P. australis	−2	2	2	46	4	6	−197	2	6	−194	6	2	−160	6	2	−11	2	2	51	2	6	−192	4	6	−176	1	2	−141	1	2
		S. lacustris	5	2	1	52	1	3	−186	11	3	−224	1	1	−191	1	1	4	1	1	28	5	3	−235	4	3						
		T. angustifolia	5	4	2	53	5	6	−197	3	6	−193	20	2	−159	20	2	−1	2	2	53	9	3	−192	2	3	−166	21	2	−131	21	2
TP	C_3gram.	Group average	5	2	5	45	5	5	−202	11	5	−201	13	5	−167	13	5	−1	3	5	43	6	5	−213	10	5	−195	15	4	−159	15	4
		C. longus (C_4)	1	2	1	44	1	3	−179	3	3	−156	1	1	−120	1	1	3	1	3	43	4	8	−147	8	8	−175	4	3	−140	4	3
		E. fluviatile	12	2	1	33	5	3	−160	4	3	−199	1	1	−164	1	1													−149 *	1	1
		N. alba																					−159	5	3						
		P. australis	−7	2	1	27	6	3	−212	4	3	−203	4	1	−170	2	1	−6	2	1	54	5	3	−203	2	3	−162	2	1	−119	1	1
		S. lacustris	24	2	1	66	5	3	−200	12	3	−216	4	1	−183	2	1															
		T. angustifolia	32	2	1	55	3	3	−211	6	3	−166	4	1	−131	2	1															
		Group average	16	12	3	49	12	3	−208	4	3	−195	15	3	−161	16	3	−6	2	1	54	5	1	−203	2	1	−162	2	1	−119	1	1
		C. longus (C_4)	13	2	1	33	6	3	−194	5	3	−194	4	1	−161	2	1															

$\varepsilon_{soilw\text{-}stw}$ is calculated between a season-site pooled value of soil water δ^2H (see Table 3A) and average species-specific δ^2H values of lower stem water; $\varepsilon_{stw\text{-}lw}$ is calculated between average species-specific δ^2H values of lower stem water and leaf water (see Table 3B). ^{2}H-fractionation values between internal water and plant *n*-alkanes ($\varepsilon_{lw\text{-}lwax}$, $\varepsilon_{lw\text{-}stwax}$, $\varepsilon_{stw\text{-}stwax}$) are calculated using an average value of all (not a subset) leaf/stem water δ^2H pooled per site and season, and a species-specific average value of leaf/stem *n*-alkane δ^2H, also pooled per site and season. All ε values are reported in permil (‰) as well as their propagated uncertainty (as a standard error of the mean; SEM); "group average" indicates a simple arithmetic mean of the average values of all species within the group.

10.3389/feart.2024.1359157

plant community as a whole, the average δ^2H_{stw} is representative of the δ^2H_{soilw} for both seasons and sites (Figure 5). Moreover, δ^2H_{soilw} has been previously linked to the local mean annual δ^2H_p (see Section 4.2.1). This demonstrates that the initial source of biosynthetic hydrogen within the plants (δ^2H_{stw}) at both sites isotopically reflects mean annual precipitation, with an at least annual integration or smoothening of the seasonal differences of the δ^2H_p signal, a conclusion comparable to findings reported in similar studies (e.g., Eensalu et al., 2023). Consequently, any intra- and inter-specific δ^2H_{wax} variability will primarily result from differences in physiology (e.g., growth form) and/or environmental conditions (e.g., aridity) during the growing season, affecting the internal processes of the plants (e.g., Griepentrog et al., 2019).

4.2.3 Lower stem water to leaf water

Generally, δ^2H_{lw} values exhibited greater enrichment in summer compared to spring (Table 3). In most species, the difference between spring and summer δ^2H_{lw} closely mirrored the seasonal variation in δ^2H_{stw} (ca. 5‰–10‰). *M. aquatica* also conformed to this pattern when a single clear outlier (−72‰) was excluded from the summer mean. The seemingly distinct behaviour of *S. lacustris* (ca 10‰ more depleted in summer) can be attributed to a sampling bias: its morphology posed challenges in clearly separating stem and leaf sections in the summer specimens. Similarly, the significant seasonal difference in *E. fluviatile* δ^2H_{lw} (ca 36‰ more negative in summer) is likely linked to the different physiology of this genus, which produces green photosynthesising stems and leaves in spring while new, low photosynthesising stems, crowned by a spore-bearing cone, emerge in summer (the latter were, in fact, sampled as "whole").

The ^{2}H-fractionation between lower stem and leaf water ($\varepsilon_{stw\text{-}lw}$; +27‰ to +60‰; Table 4) tends to be greater in species with greater height, such as *P. australis*, *T. angustifolia,* and *C. mariscus* (notably, *Cladium jamaicense* in the Florida Everglades also showed very depleted δ^2H_{lwax} values, −231‰; He et al., 2020), and relatively broader, more exposed leaves (as in *C. palustris*), potentially indicating increased evapo-transpiration.

It is important to note that our dataset offers a discrete rather than continuous representation of internal water δ^2H, a parameter that has been found to exhibit considerable variability, with seasonal to hourly fluctuations (Sachse et al., 2009, 2010). Our sampling approach captures only selected "snapshots" of stem/leaf water δ^2H distributed over a few days in spring and summer. Nevertheless, our $\varepsilon_{stw\text{-}lw}$ values demonstrate consistency between spring (+44.7‰ ± 12‰) and summer (+45.2‰ ± 10‰) species-specific averages. This stability aligns with findings in studies involving a limited number of tundra vascular plant species in western Greenland (σ=12‰; Berke et al., 2019) and suggests a levelling out of the considerable variability in stem/leaf evapo-transpiration over the extended time frame of the entire vegetative season.

4.3 Water to *n*-alkanes ^{2}H-fractionation

4.3.1 Leaf water to leaf *n*-alkanes

The ^{2}H-fractionation from leaf water to leaf *n*-alkanes ($\varepsilon_{lw\text{-}lwax}$) is known to present high specific variability. While interspecific variability is predominantly associated with differences in plant physiology, intraspecific variability (up to ca. 70‰) is attributed to diurnal/seasonal variability of leaf water δ^2H values (Sachse et al., 2012). Given these considerations, the study of $\varepsilon_{lw\text{-}lwax}$ (as well as $\varepsilon_{stw\text{-}stwax}$) tipically requires high frequency discrete sampling, ideally approximating continuous sampling, of leaf/stem water and wax *n*-alkanes throughout the entire vegetative period (e.g., Kahmen et al., 2013; Tipple et al., 2013; Newberry et al., 2015; Sachse et al., 2015).

As previously mentioned (see Section 4.2.3), our study does not rely on such continuous sampling, but rather adopts a more sporadic approach. Nevertheless, our sampling occurred during the main arc of the day, over an average of 2-3 consecutive days per season and site (see Section 2.2). To mitigate the uncertainty inherent in the sporadic sampling of individual specimens, we aggregated the leaf and lower stem water δ^2H values of all samples (395), without regard to species, computing season and site averages for δ^2H_{lw} and δ^2H_{stw} (Table 3). We regard these averages as robust estimates of community-wide δ^2H_{lw} and δ^2H_{stw} during spring and summer (Feakins and Sessions, 2010; Sachse et al., 2010). Utilising these consolidated values (Table 3B) and species-specific averages of δ^2H_{lwax} and δ^2H_{stwax} (CWMA), we derived species-specific ^{2}H-fractionation values from lower stem water to leaf water ($\varepsilon_{stw\text{-}lwax}$), leaf water to leaf wax ($\varepsilon_{lw\text{-}lwax}$), stem water to stem wax ($\varepsilon_{stw\text{-}stwax}$), and leaf water to stem wax ($\varepsilon_{lw\text{-}stwax}$), during growth and maturity seasons (Table 4).

At Nisí, especially in summer (Supplementary Table S3), C_3 graminoids showed significantly greater $\varepsilon_{lw\text{-}lwax}$ (average of species-specific mean values: spring −202‰ ± 11‰, summer −213‰ ± 10‰) than forbs (spr. −195‰ ± 8‰, sum. −176‰ ± 11‰; Table 4). The resulting $\varepsilon_{lw\text{-}lwax}$ difference between C_3 graminoids and forbs in summer (i.e., at the end of the growing season; 36‰ ± 15‰) closely mirrors the reported difference in net fractionation between the same groups (37‰ ± 42‰; Sachse et al., 2012). The larger associated error with net fractionation (±42‰) suggests that, while biosynthetic fractionation may tend to a stable mean value within plant groups, much of uncertainty in net fractionation likely stems from variations in environmental conditions affecting the water pool (δ^2H_p/δ^2H_{soilw}/δ^2H_{stw}/δ^2H_{lw}).

4.3.2 Leaf and lower stem water to lower stem *n*-alkanes

The δ^2H values of *n*-alkanes in stem samples did not exhibit a discernible seasonal pattern and our δ^2H_{stwax} values were relatively similar to the δ^2H_{lwax} values of their leaf counterpart (although often slightly less depleted; Figure 4). $\varepsilon_{stw\text{-}stwax}$ values tended to be lower than $\varepsilon_{lw\text{-}lwax}$ and displayed significant variability (Figure 7; Table 4). However, when δ^2H_{lw} is used instead of δ^2H_{stw}, the resulting $\varepsilon_{lw\text{-}stwax}$ values are much closer to $\varepsilon_{lw\text{-}lwax}$ than $\varepsilon_{stw\text{-}stwax}$ (Figure 7).

Our proposed explanation for the higher similarity between $\varepsilon_{lw\text{-}stwax}$ and $\varepsilon_{lw\text{-}lwax}$ (than between $\varepsilon_{stw\text{-}stwax}$ and $\varepsilon_{lw\text{-}lwax}$) involves a shared substrate for the *n*-alkanes synthesis between lower stems and leaves. Due the low photosynthetic activity at the base of the stem (Brazel and Ó'Maoileídigh, 2019 and refs. therein), *n*-alkanes produced there must derive their hydrogen (at least partially) from a substrate previously synthetised in leaves (Sessions, 2006; Shepherd and Griffiths, 2006). The δ^2H of this substrate would be marked by δ^2H_{lw}, used locally and then transported down to other parts of the plant, influencing the δ^2H value of locally produced *n*-alkanes, especially in organs less exposed to light (as, in our case, the base of

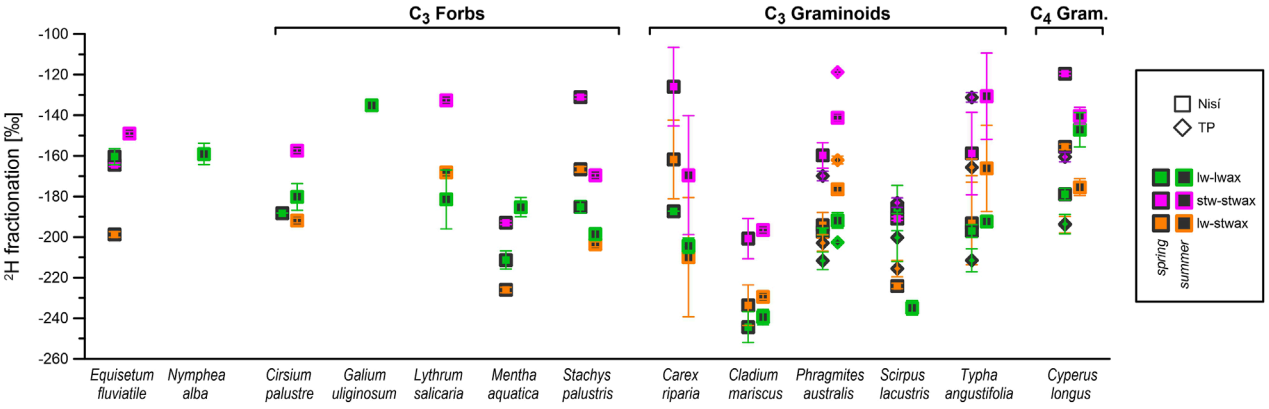

FIGURE 7
Mean ^{2}H-fractionation between 1) leaf water and *n*-alkanes (green), 2) lower stem water and *n*-alkanes (purple), 3) leaf water and lower stem *n*-alkanes (orange), for all sampled species at both sites, in spring and summer. The values of lower stem and leaf water δ^{2}H are a pooled mean for all species per each season and site (Table 3; Table 4). Vertical bars indicate propagated SEM.

the stem). This would explain both the more stable relationship of $\delta^{2}H_{stwax}$ to $\delta^{2}H_{lw}$ ($\varepsilon_{lw\text{-}stwax}$) compared to $\delta^{2}H_{stw}$ ($\varepsilon_{stw\text{-}stwax}$), as well as $\delta^{2}H_{stwax}$ slightly less depleted values compared to $\delta^{2}H_{lwax}$, as the substrate delivered to the stem would be ^{2}H-enriched after part of ^{1}H was preferentially removed by biosynthetic ^{2}H-fractionation during the synthesis of leaf wax compounds.

This proposed mechanism closely parallels to the one employed to explain less depleted $\delta^{2}H_{lwax}$ at the base of some monocot and eudicot leaves (Gao et al., 2015). It potentially aligns with other findings indicating that the δ^{2}H values of *n*-alkanes in leaves are more positive than in stems and more negative than in roots (Gamarra and Kahmen, 2015; He et al., 2020). The $\delta^{2}H_{wax}$ of those stems, exposed to light, would be influenced by the more negative $\delta^{2}H_{stw}$, unlike our lower stem samples (confined to the section close to the roots), relying more on leaf-synthesised substrate. However, another study (Liu J. et al., 2019) found $\delta^{2}H_{wax}$ to be more negative in roots than leaves in two C_3 species (*Artemisia vestita*–monocot, and *Stipa bungeana*–eudicot), and *vice versa* in *Bothriochloa ischaemum*, a C_4 monocot species. This underscores the necessity of gathering additional data on plant organs other than leaves to elucidate the variability in $\delta^{2}H_{wax}$ between different plant sections.

4.4 Net ^{2}H-fractionation

Studies on the leaf *n*-alkane ^{2}H-composition of graminoids and forbs in wetland helophytic communities are limited, with most focused on the highlands of China (Duan et al., 2014; Zhao et al., 2018; Huang and Meyers, 2019; Liu et al., 2023). It is important to note that the degree to which our net fractionation ranges ($\varepsilon_{C29/MAP}$; C_3 graminoids, summer, −207‰ to −168‰, average −182‰; C_3 forbs, summer, −156‰ to −92‰, average −145‰; Table 5) overlap to the one from other locations might have limited significance. For example, the net-fractionation values for four Chinese macroregions (Liu et al., 2023) show inconsistent overlapping to our monocot and dicot $\varepsilon_{C29/MAP}$ ranges, across different environments and climatic regions. This could derive from variations in sampled species and climatic/geographical conditions. Nevertheless, interesting similarities exist in the ^{2}H data between some Chinese sites and our Greek locations. For instance, the CMWA $\delta^{2}H_{lwax}$ values range at lake Gahai (−205‰ to −192‰) for two emergent C_3 forbs in summer (*Knorringia sibirica* and *Hippuris vulgaris*; Duan et al., 2014) falls within the interval observed in our summer forb data (−205‰ to −141‰, species specific; Table 4). Interestingly, the range for all plants from aquatics to trees (−246‰ to −130‰; Duan et al., 2014) is the same we have for just emergent plants (−251‰ to −138‰, graminoids and forbs, summer), probably due to an under sampling of helophytes at Gahai. The net fractionation also aligns, with *P. sibirica* and *H. vulgaris* showing a $\varepsilon_{C29/MAP}$-$\varepsilon_{C27/MAP}$ range (−163‰ to −141‰) substantially matching our $\varepsilon_{C29/MAP}$ range for forbs (−171‰ to −147‰, excluding *G. uliginosum* −92‰) in summer. However, correlations between more enriched $\delta^{2}H_{lwax}$ and greater leaf surface area or higher ACL, suggested in previous studies, do not hold for our data, neither for forbs (e.g., *G. uliginosum* shows the most enriched $\delta^{2}H_{lwax}$ while having much smaller leaves than other sampled forb species), nor graminoids.

More interesting is the comparison with Dajiuhu peatland data (Zhao et al., 2018) which is facilitated by the fact that the analysed emergent C_3 graminoid species belong to the same families as ours (Poaceae, Typhaceae, Cyperaceae, and, in one case, the same genus *Carex*). In Dajiuhu, the $\delta^{2}H_{lwax}$ range for emergent C_3 graminoids (−253‰ to −165‰) substantially matches ours (−256‰ to −170‰; summer) when all *n*-$C_{23\text{-}33}$ odd homologues are considered; less overlap occurs when only *n*-C_{29} values are considered (−240‰ to −213‰ in Dajiuhu, −252‰ to −176‰ in Nisí-TP). Even as the OIPC $\delta^{2}H_{MAP}$ for Dajiuhu (−70‰) and Nisí-TP (−51‰) show a ca. 20‰ difference, the average $\varepsilon_{C29/MAP}$ values for C_3 graminoids coincide (Dajiuhu −171‰, Nisí-TP -175‰; Table 5). Dajiuhu's climate is monsoonal (and not Mediterranean), with heavy, ^{2}H-depleted precipitation during late June and early July, followed by hot and dry summers (Zhao et al., 2018). However, the Dajiuhu and Nisí-TP sites are characterised by similar wetland environments

TABLE 5 Net ^{2}H-fractionation from OIPC 3.1 δ^2H_p values of mean annual precipitation (MAP) to leaf wax *n*-alkane δ^2H values, calculated for just *n*-C_{29} ($\varepsilon_{C29/MAP}$) and for the concentration weighted mean of *n*-alkanes ($\varepsilon_{CMWA/MAP}$).

			$\varepsilon_{C29/MAP}$			$\varepsilon_{CMWA/MAP}$			$\varepsilon_{C29/MAP}$			$\varepsilon_{CMWA/MAP}$		
			Mean	σ	n	Mean	σ	n	Mean	σ	n	Mean	σ	n
Nisí fen	C_3 forbs	*C. palustris*	−155	2	3	−155	2	3	−147	8	3	−143	12	3
		G. uliginosum							−92	3	3	−96	4	3
		L. salicaria							−151	33	3	−144	26	3
		M. aquatica	−177	7	3	−179	8	3	−166	15	4	−148	10	4
		S. palustris	−151	4	3	−152	5	3	−171	8	3	−162	5	3
		Group average	−161	8	3	−162	9	3	−145	14	5	−139	11	5
	C_3graminoids	*C. riparia*	−156	38	6	−154	35	6	−169	11	7	−168	10	7
		C. mariscus	−214	20	6	−214	19	6	−207	5	3	−205	7	3
		P. australis	−168	3	6	−165	3	6	−168	7	6	−155	9	6
		S. lacustris	−140	8	3	−153	20	3	−196	6	3	−200	6	3
		T. angustifolia	−172	8	6	−164	7	6	−169	5	3	−156	3	3
		Group average	−170	12	5	−170	11	5	−182	8	5	−177	11	5
	C_3gram.	*C. longus* (C_4)	−145	5	3	−146	5	3	−119	16	8	−109	25	7
		E. fluviatile	−123	8	3	−126	7	3						
		N. alba							−119	8	3	−121	9	3
TP		*P. australis*	−162	8	3	−162	8	3	−144	8	3	−141	7	3
		S. lacustris	−129	20	3	−145	7	3						
		T. angustifolia	−167	15	3	−163	16	3						
		Group average	−153	12	3	−157	6	3						
		C. longus (C_4)	−142	2	3	−138	4	3						
C_3 graminoids average			−163	25	9	−165	21	9	−175	23	7	−171	26	7

All values are in permil unit (‰).

as well as a similar relationship between vegetative period and seasonality, even if in Dajiuhu this is shifted later into summer.

These data show that, while fractionation values may vary greatly between individuals of similar species and sampling instances, a certain integration occurs when the plant communities are considered in their entirety. In particular, they suggest that net fractionation may be relatively constant (Liu et al., 2023) in similar C_3 graminoids helophytic communities, regardless of absolute differences in precipitation δ^2H and temperature, as long as (1) the relationship between growing season and precipitation/aridity periods is similar (as between Nisí-TP and Dajiuhu), and (2) the source water δ^2H selected to calculate net fractionation actually reflects the real source water δ^2H in the local environment (Yu et al., 2021).

However, it should be noted that other studies incidentally show very similar $\varepsilon_{C29/MAP}$ values for C_3 graminoid helophytes (*P. australis*, −166‰, Qiushui valley, Liu et al., 2017; *Typha latifolia*, −150‰, Blood Pond, Hou et al., 2007a) or even just C_3 graminoids (Smith and Freeman, 2006; Hou et al., 2007a; Oakes and Hren, 2015; Daniels et al., 2017; Freimuth et al., 2019), without sharing similar climatic conditions and/or species families.

Unfortunately, the same level of comparison between Dajiuhu and Nisí-TP can not be achieved with C_3 forbs species belonging to different families ($\varepsilon_{C29/MAP}$ Dajiuhu −110‰, Nisí-TP -145‰ summer; Table 5). However, both studies report net fractionation to decrease (from more negative to less negative) from graminoids to forbs (Zhao et al., 2018; Liu et al., 2023). Other studies involving vascular plants in wetland environments generally report lower (less

negative) $\varepsilon_{C29/MAP}$ values. Both graminoids (n=2) and forbs (n=2) from the Northern Norwegian Hollabåttjønnen bog show extremely low values (−53‰ if δ^2H_{MAP} or −93‰ if July δ^2H for graminoids, −71‰ if δ^2H_{MAP}, −110‰ if July δ^2H for forbs; Balascio et al., 2018), as well as *P. australis* from the East Anglian Stiffkey saltmarshes (−144‰; Eley et al., 2014). The same *P. australis* in Stockholm, Sweden shows lower $\varepsilon_{C29/MAP}$ values (−132‰, only 1 data-point; Yang et al., 2011) and substantially lower values (−95‰) from three high altitude sites along a latitudinal gradient in inner China (Duan and He, 2011). This is a reminder that, although wetland helophytes (particularly C_3 graminoids) appear to tend toward a stable net fractionation value, other factors such as, for example, higher latitude effects on seasonality and growing season (Yang et al., 2011; Daniels et al., 2017; Balascio et al., 2018; Corcoran et al., 2022), salinity effects (Eley et al., 2014; Ceccopieri et al., 2021) and elevation (Duan and He, 2011), must be taken into account when attempting any kind of δ^2H_p reconstruction from sedimentary δ^2H_{wax} from wetlands.

4.5 Seasonal differences in the δ^2H values of odd/even homologues

Odd numbered *n*-alkanes consistently exhibited more ^2H-depletion than their adjacent even carbon numbered counterparts, with few exceptions (Figure 3). This pattern does not appear to be an analytical artefact, as (1) we assessed only peaks over 2 Vs and corrected for peak area values lower than 40 Vs (see Supplementary Material S1, Supplementary Figure S1), (2) it is evident also in samples where even homologues concentrations occasionally match or exceed odd homologues concentrations, and (3) it aligns with the findings of previous studies on leaf wax *n*-alkanes, *n*-alkanols, *n*-aldehydes and *n*-fatty acids in higher plants (e.g., Collister et al., 1994; Yang and Huang, 2003; Chikaraishi et al., 2004a; Sachse et al., 2006; Hou et al., 2007b).

To quantify and characterise this odd/even ^2H-composition pattern, we devised a Parity Isotopic Difference index (PID; see Section 2.4). PID values (Table 6), ranging from −20 to 51, are almost always positive (except for *C. riparia*, *C. palustre* and *T. angustifolia* in spring) indicating consistently lower δ^2H values for *n*-alkane even homologues. Interestingly, PID values are also consistently higher in summer samples (an increase between +12 and +70 relative to spring values), with the only exception of *M. aquatica* and *S. palustris*. The PID average (all species) is significantly (ca 6 times; Supplementary Table S3) higher in summer than in spring, indicating a spring to summer increase in the difference between odd and even δ^2H_{lwax} values.

The cause of this behaviour is currently unknown. Drawing from prior investigations (Zhou et al., 2010; Eley et al., 2018), we posit that either environmental factors (e.g., aridity) or physiological influences may have affected the a) ^2H-composition of pyruvate, the precursor to both odd and even *n*-alkane homologues, and/or b) the availability of pyruvate from different sources (e.g., NADPH, carbohydrates; Schmidt et al., 2003; Ladd and Sachs, 2012). The production of *n*-alkanes is predominantly driven by odd-numbered homologues through the pyruvate-acetate pathway, and primarily utilises strongly ^2H-depleted NADPH derived pyruvate (Schmidt et al., 2003). However, a drought related increase in lipid metabolism, which would also lead to an uptick in even-numbered *n*-alkanes production (which would result also in strongly decreasing CPI values; see Section 4.1.2), could potentially enhance the use of the pyruvate-propionate pathway for the synthesis of even-homologues (Zhou et al., 2010), tapping into less ^2H-depleted sources of hydrogen (e.g., pyruvate from carbohydrates or leaf water; Eley et al., 2018), creating a discernible differential fractionating effect on these distinct biosynthetic pathways, and thus be also recorded as a shift in PID.

Interestingly, our data revealed a notable monotonic anti-correlation of PID with plant CPI (Spearman $\rho = -0.625$, $p = 0.001$; Kendall $\tau = -0.492$, $p = 0.001$), which also varies seasonally (see Section 4.1.2). This inverse correlation is evident (Figure 8) across all species, apart from *M. aquatica* and *S. palustris*, where seasonal differences in PID and CPI are minimal and can be considered substantially unaltered. The strong correlation with CPI suggests that the PID records a genuine signal, likely arising from seasonal difference in the production of even-homologues.

However, due to the low temporal resolution of our data (only spring/summer, each represented by one data-point) and the absence of comparable data from other studies, we lack sufficient data for a conclusive outcome on this matter. Nevertheless, we can speculate on a new hypothetical proxy mechanism involving both CPI and PID. Seasonal variations in plant CPI suggests that shifts in aridity during the vegetative season consistently modify the production of *n*-alkane even and odd homologues. Despite the lack of a reliable correlation between plant CPI and soil/sediment CPI, as discussed above (4.1.2), due to preferential degradation of longer homologues and microbial activity (Thomas et al., 2021; Corcoran et al., 2022 and refs therein), assuming that the same degradation processes do not modify the ^2H-composition of *n*-alkanes in soil/sediment, the correlation between PID and aridity (and thus also CPI) could potentially be reliable.

The PID index might become a valuable proxy for qualitatively tracing aridity shifts during the growing season of the plant community that contributed to the sedimentary archive. Should these seasonal relationships between CPI and PID, along with the absence of additional ^2H-fractionation in sediment, be substantiated through specific studies, it may introduce innovative approaches to qualitatively discern long-term aridity variations within sedimentary paleo-archives. Nevertheless, further research is essential to uncover its origin and assess its applicability for paleo-applications.

5 Conclusion

In order to better understand the environmental and plant physiological controls of *n*-alkanes as biomarkers in sedimentary archives originated from wetlands, we analysed specific and seasonal variations of (1) *n*-alkane concentration, distribution, and hydrogen isotopic composition, and (2) ^2H-fractionation steps from source water to wax *n*-alkanes, in leaves/stems of several species from a Mediterranean helophytic plant community.

Based on our concentration data and resulting average chain length index values, it appears that local graminoid species are the predominant source of the local soil *n*-alkane signal, with a lesser contribution from forbs. This might be attributed to

10.3389/feart.2024.1359157

TABLE 6 Values of PID (Parity Isotopic Difference index) and CPI (Carbon Preference Index) from leaf wax *n*-alkanes per each species, divided by site and season.

		PID				CPI			
		Nisí fen		TP		Nisí fen		TP	
		Spring	Summer	Spring	Summer	Spring	Summer	Spring	Summer
C_3 forbs	*C. palustre*	−14	66			58.4	14.7		
	G. uliginosum		21				19.1		
	L. salicaria		16				8.7		
	M. aquatica	15	8			7.7	8.8		
	S. palustris	13	14			10.5	8.7		
C_3 graminoids	*C. riparia*	−19	25			26	18.3		
	C. mariscus	23	33			15.5	6.9		
	P.s australis	9	52		11	17.6	4.5	27.2	20.6
	S. lacustris	14		30		5.3	52.5	6.9	
	T. angustifolia	6	44	10		13.2	2.8	13.9	
	C. longus (C_4)		42			23.2	2.8	26.5	
	E. fluviatile	13	35			11.6	6.6[a]		
	N. alba		45				3.6		

[a]Values referring to "whole" *E. fluviatile* fertile shoot samples.
Higher absolute PID values indicate higher δ^2H_{lwax} average difference between odd and even homologues; positive values indicate that odd homologues are averagely more ^2H-depleted than even homologues, and vice versa. A visualisation of the apparent inverse relationship between PID and CPI is reported in Figure 8.

differences in morphology and vegetation structure between these two plant groups.

Our data reveal that the δ^2H values of surface and soil water collected between spring and summer align with the local average annual precipitation δ^2H signal, which, in turn, closely reflects the weighted average δ^2H of winter-spring precipitation derived from available stations data. Furthermore, we observe a consistent agreement in the average δ^2H of local surface water, soil water, and stem water, indicating little to no evaporative enrichment of soil water relative to winter-spring precipitation, and confirming negligible ^2H-fractionation in the root-stem during water uptake, as previously reported in the literature. Overall, these findings confirm that the δ^2H values of the source water accessible to local fen plant communities for wax compounds synthesis indeed reflect the δ^2H of annual precipitation, underscoring the potential of δ^2H of local plant derived *n*-alkanes as tracer of long-term seasonality shifts.

Specifically, our concentration and distribution data indicate that, consistently with similar studies in other environments, the primary source of the local sedimentary *n*-alkane signal derives mainly from the leaves of local fen plants. However, this leaf-stem difference appears to have minimal impact in terms of the δ^2H signal. In fact, as anticipated, while leaf water exhibits higher ^2H-enrichment compared to stem water, indicative of transpirative enrichment in the leaf water pool, we observe comparable *n*-alkane δ^2H values between lower stems and leaves. This similarity implies that the production of wax compounds in both organs relies on a shared metabolic substrate, likely originating in leaves and synthesised from leaf water.

While we detect significant inter- and intra-specific variability in leaf wax δ^2H and related net ^2H-fractionation, when integrated at a community level, we noticed a general tendency to stabilise toward known average values from literature, particularly when it comes to plant forms. Compared to studies conducted in similar environments worldwide, our average net ^2H-fractionation values (between precipitation and leaf *n*-alkanes) still rank among the most negative, but this is likely due to a combination of plant typology (grasses) and random differences in the selection of species sampled. However, the C_3 forbs δ^2H values for *n*-C_{29} (−152‰ ± 27‰) align with those reported for comparable wetland environments in the Chinese highlands, as do C_3 graminoids values (−170‰ ± 26‰), which mirror findings from other studies in similar settings. This similarity suggests relatively consistent net fractionation values for these peri-lacustrine/fen communities not only in the Mediterranean but also in other climatic zones, provided similar seasonality and absence of particular skewing factors (e.g., higher latitude seasonality, salinity). Overall, this means that if information on the main constraining factors is known,

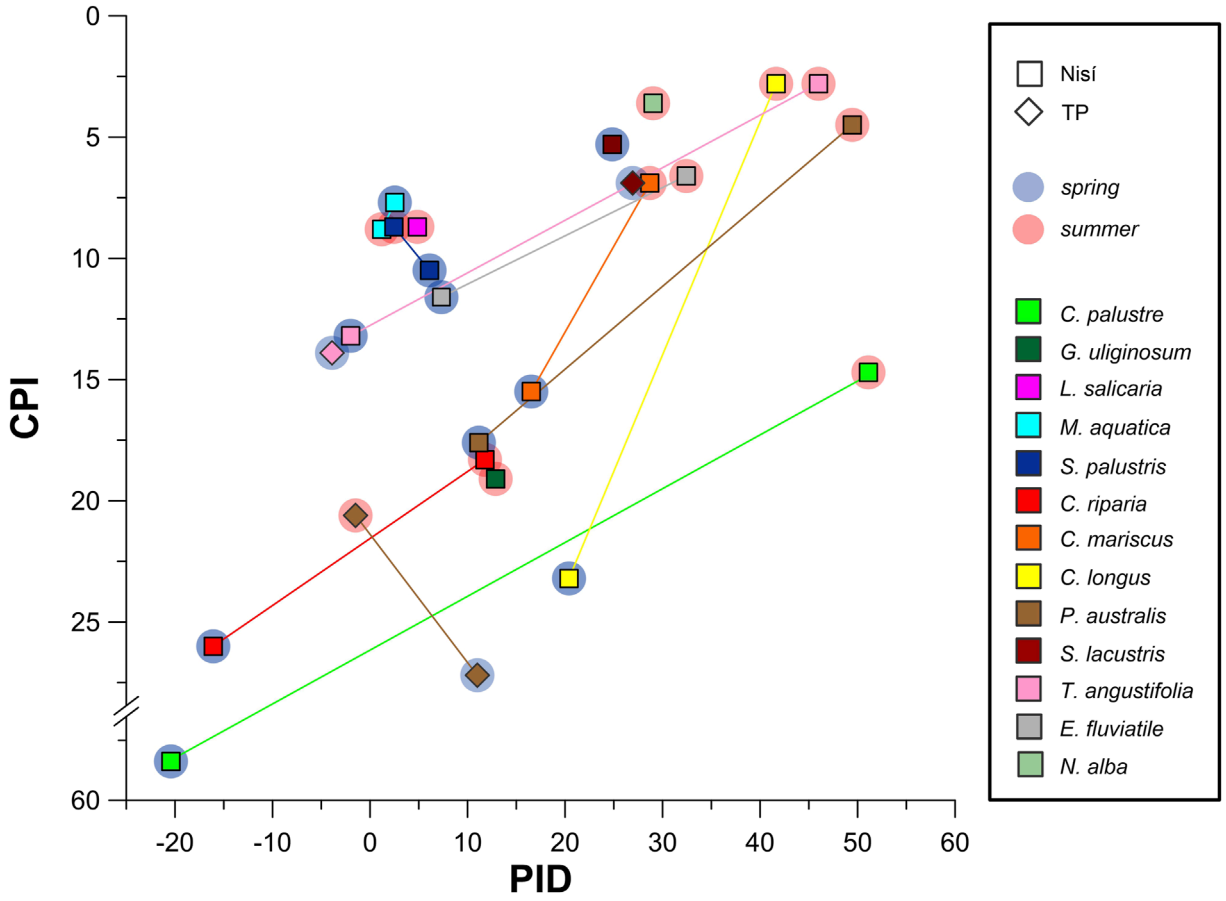

FIGURE 8
PID (Parity Isotopic Difference index) and CPI (Carbon Preference Index) cross-plot. Spring and summer values (when both available) for the same species and site are connected by a straight line. All paired values show a PID increase and a CPI decrease from spring to summer (except *Phragmites australis* in TP and *Stachys palustris*). Interestingly, PID (and often CPI too) of the few species with available data show virtually the same values in Nisí and TP during spring (*Scirpus lacustris*, *Phragmites australis*, *Typha angustifolia*.

these helophytic communities could potentially provide an accurate estimate (at least qualitative) of net ^{2}H-fractionation between δ^2H_p to δ^2H_{wax}, particularly when this signal is then buried into the sediment and integrated over longer time scales.

In the Mediterranean context, any future attempt to use δ^2H_{wax} from lacustrine/palustrine sedimentary archives as a paleo-precipitation proxy should consider factors, such as the long-term stability of graminoid dominance and of their net ^{2}H-fractionation value to trace any change in precipitation patterns that would result from the local climate shifting away from typical Mediterranean conditions. In particular, the interpretation of the δ^2H *n*-alkane patterns of the TP sedimentary record (Ardenghi et al., 2019) rely on the assumptions that (1) the long term shift in *n*-alkane δ^2H does not derive from a shift in the composition of the local plant community, and that (2) plant derived *n*-alkane δ^2H is a reliable proxy for the source water of local plants. Our data seem to confirm both points, as (1) local graminoids (more common during colder periods; Pross et al., 2015) present greater net fractionation than forbs, and (2) leaf *n*-alkane δ^2H values show to be a reliable proxy for source plant water δ^2H in the local community.

Our data also highlights a consistent decrease from spring to summer of the carbon preference index (CPI) in plant samples, pointing toward seasonal changes in wax lipid synthesis, likely linked to increased drought. Unfortunately, generally lower soil CPI values, likely due to non-homogeneous microbial production and degradation of *n*-alkane homologues, show that this seasonal signal seems can not be traced through the analysis of soil/sediment CPI.

However, another seasonal pattern emerged from our data: we observed a distinct and consistent ^{2}H-difference between odd- and even-numbered *n*-alkanes (less and more depleted, respectively) in our plant samples. To quantify this, we introduced a new parity isotopic difference index (PID). The PID consistently increases from spring to summer, indicating a seasonal environmental or physiological influence associated with increased production of even homologues, implying a possible differential ^{2}H-fractionation between the biosynthetic pathways of odd and even *n*-alkane homologues. This PID seasonal pattern also exhibits a clear inverse correlation to CPI. While we lack sufficient data for a conclusive outcome on this matter, if these seasonal relationships of CPI and PID are validated in specific studies, it could potentially open new avenues to trace long term qualitative aridity shifts through

the analysis of the δ^2H in odd and even *n*-alkane homologues in sedimentary archives.

Data availability statement

All raw data will be available on the Pangaea database (https://www.pangaea.de/). The data will also be made available upon request.

Author contributions

NA: Conceptualization, Data curation, Formal Analysis, Investigation, Methodology, Project administration, Validation, Visualization, Writing–original draft, Writing–review and editing, Software. AM: Funding acquisition, Resources, Supervision, Writing–review and editing. JM: Software, Writing–review and editing. DS: Writing–review and editing. AK: Methodology, Resources, Writing–review and editing. EN: Conceptualization, Funding acquisition, Investigation, Methodology, Project administration, Resources, Supervision, Writing–review and editing.

Funding

The author(s) declare that financial support was received for the research, authorship, and/or publication of this article. Financial support by the Senckenberg Biodiversity and Climate Research Centre (SBiK-F) is gratefully acknowledged.

Acknowledgments

We thank Dr. Elissavet Dotsika and Dr. Stavros Kalaitzidis for sharing with us their knowledge on Greek peatlands and isotopic hydrology, and Patrick Nowara and Dr. Paraskevi Chantzi for their invaluable help during the field campaign. We thank Ulrich Treffert for his invaluable laboratory support, as well as Dr. Daniel Nelson, Dr. Sarah Newberry, and Dr. Victor Evrard for their fundamental help to processing and analysing our samples at the Basel University botanical laboratories.

Conflict of interest

The authors declare that the research was conducted in the absence of any commercial or financial relationships that could be construed as a potential conflict of interest.

The handling editor MR-G declared a past Authorship with one of the authors DS.

The author(s) declared that they were an editorial board member of Frontiers, at the time of submission. This had no impact on the peer review process and the final decision.

Publisher's note

Supplementary material

The Supplementary Material for this article can be found online at: https://www.frontiersin.org/articles/10.3389/feart.2024.1359157/full#supplementary-material

References

Anderson, D., Goudie, A., and Parker, A. (2013). *Global environments through the quaternary*. Oxford: Oxford University Press. doi:10.1093/acprof:osobl/9780199697267.001.0001

Ardenghi, N., Mulch, A., Koutsodendris, A., Pross, J., Kahmen, A., and Niedermeyer, E. M. (2019). Temperature and moisture variability in the eastern Mediterranean region during Marine Isotope Stages 11–10 based on biomarker analysis of the Tenaghi Philippon peat deposit. *Quat. Sci. Rev.* 225, 105977. doi:10.1016/j.quascirev.2019.105977

Ardenghi, N., Mulch, A., Pross, J., and Maria Niedermeyer, E. (2017). Leaf wax *n*-alkane extraction: an optimised procedure. *Org. Geochem.* 113, 283–292. doi:10.1016/j.orggeochem.2017.08.012

Arp, G., Thiel, V., Reimer, A., Michaelis, W., and Reitner, J. (1999). Biofilm exopolymers control microbialite formation at thermal springs discharging into the alkaline Pyramid Lake, Nevada, USA. *Sediment. Geol.* 126, 159–176. doi:10.1016/S0037-0738(99)00038-X

Bai, Y., Azamdzhon, M., Wang, S., Fang, X., Guo, H., Zhou, P., et al. (2019). An evaluation of biological and climatic effects on plant *n*-alkane distributions and δ^2H_{alk} in a field experiment conducted in central Tibet. *Org. Geochem.* 135, 53–63. doi:10.1016/j.orggeochem.2019.06.003

Balascio, N. L., D'Andrea, W. J., Anderson, R. S., and Wickler, S. (2018). Influence of vegetation type on *n*-alkane composition and hydrogen isotope values from a high latitude ombrotrophic bog. *Org. Geochem.* 121, 48–57. doi:10.1016/j.orggeochem.2018.03.008

Barnard, R. L., De Bello, F., Gilgen, A. K., and Buchmann, N. (2006). The $\delta^{18}O$ of root crown water best reflects source water $\delta^{18}O$ in different types of herbaceous species. *Rapid Commun. Mass Spectrom.* 20, 3799–3802. doi:10.1002/rcm.2778

Berke, M. A., Sierra, A. C., Bush, R. T., Cheah, D., and O'Connor, K. (2019). Controls on leaf wax fractionation and δ^2H values in tundra vascular plants from western Greenland. *Geochim. Cosmoc. Acta* 244, 565–583. doi:10.1016/j.gca.2018.10.020

Borromei, A. M., Coronato, A., Franzén, L. G., Ponce, J. F., Sáez, J. A. L., Maidana, N., et al. (2010). Multiproxy record of Holocene paleoenvironmental change, Tierra del Fuego, Argentina. *Palaeogeogr. Palaeoclimatol. Palaeoecol.* 286, 1–16. doi:10.1016/j.palaeo.2009.11.033

Brader, A. V., van Winden, J. F., Bohncke, S. J. P. P., Beets, C. J., Reichart, G.-J. J., and De Leeuw, J. W. (2010). Fractionation of hydrogen, oxygen and carbon isotopes in *n*-alkanes and cellulose of three *Sphagnum* species. *Org. Geochem.* 41, 1277–1284. doi:10.1016/j.orggeochem.2010.09.006

Brazel, A. J., and Ó'Maoileídigh, D. S. (2019). Photosynthetic activity of reproductive organs. *J. Exp. Bot.* 70, 1737–1754. doi:10.1093/jxb/erz033

Britton, R. H., and Crivelli, A. J. (1993). "Wetlands of southern europe and north africa: mediterranean wetlands," in *Wetlands of the world: inventory, ecology and management volume I: africa, Australia, Canada and Greenland, mediterranean, Mexico, Papua New Guinea, south asia, tropical south America, United States*. Editors D. F. Whigham, D. Dykyjová, and S. Hejný (Dordrecht: Springer Netherlands), 129–194. doi:10.1007/978-94-015-8212-4_6

Bryson, C. T., and Carter, R. (2008). "The significance of Cyperaceae as weeds," in *Sedges: uses, diversity, and systematics of the Cyperaceae*, 15–101.

Buczek, A. (2005). Habitat conditions, ecology, resources and protection of saw sedge Cladium mariscus (L.) Pohl. in Lublin macroregion. *Acta Agroph* 9 (129), 1–127.

Burdick, D. M., Buchsbaum, R., and Holt, E. (2001). Variation in soil salinity associated with expansion of *Phragmites australis* in salt marshes. *Environ. Exp. Bot.* 46, 247–261. doi:10.1016/S0098-8472(01)00099-5

Bush, R. T., and McInerney, F. A. (2013). Leaf wax *n*-alkane distributions in and across modern plants: implications for paleoecology and chemotaxonomy. *Geochim. Cosmoc. Acta* 117, 161–179. doi:10.1016/j.gca.2013.04.016

Bush, R. T., and McInerney, F. A. (2015). Influence of temperature and C4 abundance on n-alkane chain length distributions across the central USA. *Org. Geochem.* 79, 65–73. doi:10.1016/j.orggeochem.2014.12.003

Butiseacă, G. A., van der Meer, M. T. J., Kontakiotis, G., Agiadi, K., Thivaiou, D., Besiou, E., et al. (2022). Multiple crises preceded the Mediterranean Salinity Crisis: aridification and vegetation changes revealed by biomarkers and stable isotopes. *Glob. Planet. Change* 217, 103951. doi:10.1016/j.gloplacha.2022.103951

Carrión, J. S., and Van Geel, B. (1999). Fine-resolution upper weichselian and holocene palynological record from navarres (valencia, Spain) and a discussion about factors of mediterranean forest succession. *Rev. Palaeobot. Palynol.* 106, 209–236. doi:10.1016/S0034-6667(99)00009-3

Ceccopieri, M., Scofield, A. L., Almeida, L., Araújo, M. P., Hamacher, C., Farias, C. O., et al. (2021). Carbon isotopic composition of leaf wax *n*-alkanes in mangrove plants along a latitudinal gradient in Brazil. *Org. Geochem.* 161, 104299. doi:10.1016/j.orggeochem.2021.104299

Chase, B. M., Niedermeyer, E. M., Boom, A., Carr, A. S., Chevalier, M., He, F., et al. (2019). Orbital controls on Namib Desert hydroclimate over the past 50,000 years. *Geology* 47, 867–871. doi:10.1130/g46334.1

Chatterjee, S., Das, S. K., Behera, P. K., Ghosh, D., Chakraborty, A., Patel, P. P., et al. (2023). Short-chain *n*-alkanes in benthic mats and mosses from the Larsemann Hills, East Antarctica. *Org. Geochem.* 179, 104587. doi:10.1016/j.orggeochem.2023.104587

Chawchai, S., Chabangborn, A., Fritz, S., Väliranta, M., Mörth, C. M., Blaauw, M., et al. (2015). Hydroclimatic shifts in northeast Thailand during the last two millennia - the record of Lake Pa Kho. *Quat. Sci. Rev.* 111, 62–71. doi:10.1016/j.quascirev.2015.01.007

Chen, G., Li, X., Tang, X., Qin, W., Liu, H., Zech, M., et al. (2022). Variability in pattern and hydrogen isotope composition (δ^2H) of long-chain *n*-alkanes of surface soils and its relations to climate and vegetation characteristics: a meta-analysis. *Pedosphere* 32, 369–380. doi:10.1016/S1002-0160(21)60080-2

Chikaraishi, Y., and Naraoka, H. (2003). Compound-specific δD-$\delta^{13}C$ analyses of *n*-alkanes extracted from terrestrial and aquatic plants. *Phytochemistry* 63, 361–371. doi:10.1016/S0031-9422(02)00749-5

Chikaraishi, Y., and Naraoka, H. (2006). Carbon and hydrogen isotope variation of plant biomarkers in a plant-soil system. *Chem. Geol.* 231, 190–202. doi:10.1016/j.chemgeo.2006.01.026

Chikaraishi, Y., Naraoka, H., and Poulson, S. R. (2004a). Carbon and hydrogen isotopic fractionation during lipid biosynthesis in a higher plant (*Cryptomeria japonica*). *Phytochemistry* 65, 323–330. doi:10.1016/j.phytochem.2003.12.003

Chikaraishi, Y., Naraoka, H., and Poulson, S. R. (2004b). Hydrogen and carbon isotopic fractionations of lipid biosynthesis among terrestrial (C_3, C_4 and CAM) and aquatic plants. *Phytochemistry* 65, 1369–1381. doi:10.1016/j.phytochem.2004.03.036

Christanis, K. (1994). The genesis of the Nissi peatland (northwestern Greece) as an example of peat and lignite deposit formation in Greece. *Int. J. Coal Geol.* 26, 63–77. doi:10.1016/0166-5162(94)90032-9

Cohen, E. R., Cvitas, T., and Frey, J. G. (2007). *IUPAC quantities, units and symbols in physical chemistry*.

Collins, J. A., Schefuß, E., Mulitza, S., Prange, M., Werner, M., Tharammal, T., et al. (2013). Estimating the hydrogen isotopic composition of past precipitation using leaf-waxes from western Africa. *Quat. Sci. Rev.* 65, 88–101. doi:10.1016/j.quascirev.2013.01.007

Collister, J. W., Rieley, G., Stern, B., Eglinton, G., and Fry, B. (1994). Compound-specific isotope analysis in biogeochemistry and petroleum research compound-specific $\delta^{13}C$ analyses of leaf lipids from plants with differing carbon dioxide metabolisms. *Org. Geochem.* 21, 619–627. doi:10.1016/0146-6380(94)90008-6

Coplen, T. B. (2011). Guidelines and recommended terms for expression of stable-isotope-ratio and gas-ratio measurement results. *Rapid Commun. Mass Spectrom.* 25, 2538–2560. doi:10.1002/rcm.5129

Corcoran, M. C., Diefendorf, A. F., Lowell, T. V., Hall, B. L., Spoth, M. M., Schartman, A., et al. (2022). Hydrogen and carbon isotope fractionation in modern plant wax *n*-alkanes from the Falkland Islands. *Org. Geochem.* 166, 104404. doi:10.1016/j.orggeochem.2022.104404

Cormier, M. A., Werner, R. A., Leuenberger, M. C., and Kahmen, A. (2019). ^2H-enrichment of cellulose and *n*-alkanes in heterotrophic plants. *Oecologia* 189, 365–373. doi:10.1007/s00442-019-04338-8

Cormier, M. A., Werner, R. A., Sauer, P. E., Gröcke, D. R., Leuenberger, M. C., Wieloch, T., et al. (2018). ^2H-fractionations during the biosynthesis of carbohydrates and lipids imprint a metabolic signal on the δ^2H values of plant organic compounds. *New Phytol.* 218, 479–491. doi:10.1111/nph.15016

Cranwell, P. A. (1984). Lipid geochemistry of sediments from Upton Broad, a small productive lake. *Org. Geochem.* 7, 25–37. doi:10.1016/0146-6380(84)90134-7

Cranwell, P. A., Eglinton, G., and Robinson, N. (1987). Lipids of aquatic organisms as potential contributors to lacustrine sediments—II. *Org. Geochem.* 11, 513–527. doi:10.1016/0146-6380(87)90007-6

Cui, J. W., Huang, J. H., and Xie, S. C. (2008). Characteristics of seasonal variations of leaf *n*-alkanes and *n*-alkenes in modern higher plants in Qingjiang, Hubei Province, China. *Chin. Sci. Bull.* 53, 2659–2664. doi:10.1007/s11434-008-0194-8

Daniels, W. C., Russell, J. M., Giblin, A. E., Welker, J. M., Klein, E. S., and Huang, Y. (2017). Hydrogen isotope fractionation in leaf waxes in the Alaskan Arctic tundra. *Geochim. Cosmoc. Acta* 213, 216–236. doi:10.1016/j.gca.2017.06.028

Dembicki, H., Meinschein, W. G., and Hattin, D. E. (1976). Possible ecological and environmental significance of the predominance of even-carbon number C_{20}-C_{30} *n*-alkanes. *Geochim. Cosmoc. Acta* 40, 203–208. doi:10.1016/0016-7037(76)90177-0

Desprat, S., Combourieu-Nebout, N., Essallami, L., Sicre, M. A., Dormoy, I., Peyron, O., et al. (2013). Deglacial and holocene vegetation and climatic changes in the southern central Mediterranean from a direct land-sea correlation. *Clim. Past.* 9, 767–787. doi:10.5194/cp-9-767-2013

Diefendorf, A. F., Bickford, C. P., Schlanser, K. M., Freimuth, E. J., Hannon, J. S., Grossiord, C., et al. (2021). Plant wax and carbon isotope response to heat and drought in the conifer *Juniperus monosperma*. *Org. Geochem.* 153, 104197. doi:10.1016/j.orggeochem.2021.104197

Diefendorf, A. F., and Freimuth, E. J. (2017). Extracting the most from terrestrial plant-derived *n*-alkyl lipids and their carbon isotopes from the sedimentary record: a review. *Org. Geochem.* 103, 1–21. doi:10.1016/j.orggeochem.2016.10.016

Dixit, Y., Toucanne, S., Lora, J. M., Fontanier, C., Pasquier, V., Bonnin, L., et al. (2019). Enhanced western Mediterranean rainfall during past interglacials driven by North Atlantic pressure changes. *Clim. Past. Discuss.*, 1–28. doi:10.5194/cp-2019-75

Dotsika, E., Lykoudis, S. P., and Poutoukis, D. (2010). Spatial distribution of the isotopic composition of precipitation and spring water in Greece. *Glob. Planet. Change* 71, 141–149. doi:10.1016/j.gloplacha.2009.10.007

Douglas, P. M. J., Pagani, M., Brenner, M., Hodell, D. A., and Curtis, J. H. (2012). Aridity and vegetation composition are important determinants of leaf-wax δD values in southeastern Mexico and Central America. *Geochim. Cosmoc. Acta* 97, 24–45. doi:10.1016/j.gca.2012.09.005

Duan, Y., and He, J. (2011). Distribution and isotopic composition of *n*-alkanes from grass, reed and tree leaves along a latitudinal gradient in China. *Geochem. J.* 45, 199–207. doi:10.2343/geochemj.1.0115

Duan, Y., Wu, Y., Cao, X., Zhao, Y., and Ma, L. (2014). Hydrogen isotope ratios of individual *n*-alkanes in plants from Gannan Gahai Lake (China) and surrounding area. *Org. Geochem.* 77, 96–105. doi:10.1016/j.orggeochem.2014.10.005

Eensalu, M., Nelson, D. B., Buczynska, A., Rach, O., Klein, E. S., Dodd, J. P., et al. (2023). Hydrogen isotope biogeochemistry of plant waxes in paired lake catchments. *Org. Geochem.* 185, 104674. doi:10.1016/j.orggeochem.2023.104674

Eglinton, G., and Hamilton, R. J. (1967). Leaf epicuticular waxes. *Sci. (80-)* 156, 1322–1335. doi:10.1126/science.156.3780.1322

Eglinton, G., and Logan, G. A. (1991). Molecular preservation. *Philos. Trans. R. Soc. Lond. Ser. B Biol. Sci.* 333, 315–327. doi:10.1098/rstb.1991.0081

Eglinton, T. I., and Eglinton, G. (2008). Molecular proxies for paleoclimatology. *Earth Planet. Sci. Lett.* 275, 1–16. doi:10.1016/j.epsl.2008.07.012

Ehleringer, J. R., and Dawson, T. E. (1992). Water uptake by plants: perspectives from stable isotope composition. *Plant, Cell Environ.* 15, 1073–1082. doi:10.1111/j.1365-3040.1992.tb01657.x

Eley, Y., Dawson, L., Black, S., Andrews, J., and Pedentchouk, N. (2014). Understanding $^2H/^1H$ systematics of leaf wax *n*-alkanes in coastal plants at Stiffkey saltmarsh, Norfolk, UK. *Geochim. Cosmoc. Acta* 128, 13–28. doi:10.1016/j.gca.2013.11.045

Eley, Y., White, J., Dawson, L., Hren, M., and Pedentchouk, N. (2018). Variation in hydrogen isotope composition among salt marsh plant organic compounds highlights biochemical mechanisms controlling biosynthetic fractionation. *J. Geophys. Res. Biogeosc.* 123, 2645–2660. doi:10.1029/2018JG004403

Esri (2023). ArcGIS pro (version 3.1.0); earthstar geographic "world imagery" map. Available at: https://www.arcgis.com/home/item.html?id=10df2279f9684e4a9f6a7f08febac2a9 (Accessed March, 2024).

Feakins, S. J., and Sessions, A. L. (2010). Controls on the D/H ratios of plant leaf waxes in an arid ecosystem. *Geochim. Cosmoc. Acta* 74, 2128–2141. doi:10.1016/j.gca.2010.01.016

Ficken, K. J., Barber, K. E., and Eglinton, G. (1998). Lipid biomarker, $\delta^{13}C$ and plant macrofossil stratigraphy of a Scottish montane peat bog over the last two millennia. *Org. Geochem.* 28, 217–237. doi:10.1016/S0146-6380(97)00126-5

Ficken, K. J., Li, B., Swain, D. L., and Eglinton, G. (2000). An *n*-alkane proxy for the sedimentary input of submerged/floating freshwater aquatic macrophytes. *Org. Geochem.* 31, 745–749. doi:10.1016/S0146-6380(00)00081-4

Fischer, T., and Wilkes, H. (2003). *Lipid biomarkers in lacustrine sedimentary archives – an inventory and evaluation as proxies for environmental and climatic change*. Germany: ETDEWEB. Fak. VI - Bauingenieurwes. und Angew. Geowissenschaften.

Freimuth, E. J., Diefendorf, A. F., and Lowell, T. V. (2017). Hydrogen isotopes of *n*-alkanes and *n*-alkanoic acids as tracers of precipitation in a temperate forest and implications for paleorecords. *Geochim. Cosmoc. Acta* 206, 166–183. doi:10.1016/j.gca.2017.02.027

Freimuth, E. J., Diefendorf, A. F., Lowell, T. V., and Wiles, G. C. (2019). Sedimentary *n*-alkanes and *n*-alkanoic acids in a temperate bog are biased toward woody plants. *Org. Geochem.* 128, 94–107. doi:10.1016/j.orggeochem.2019.01.006

Gamarra, B., and Kahmen, A. (2015). Concentrations and δ^2H values of cuticular *n*-alkanes vary significantly among plant organs, species and habitats in grasses from an alpine and a temperate European grassland. *Oecologia* 178, 981–998. doi:10.1007/s00442-015-3278-6

Gamarra, B., and Kahmen, A. (2017). Low secondary leaf wax *n*-alkane synthesis on fully mature leaves of C_3 grasses grown at controlled environmental conditions and variable humidity. *Rapid Commun. Mass Spectrom.* 31, 218–226. doi:10.1002/rcm.7770

Gamarra, B., Sachse, D., and Kahmen, A. (2016). Effects of leaf water evaporative ^2H-enrichment and biosynthetic fractionation on leaf wax *n*-alkane δ^2H values in C_3 and C_4 grasses. *Plant Cell Environ.* 39, 2390–2403. doi:10.1111/pce.12789

Gao, L., Edwards, E. J., Zeng, Y., and Huang, Y. (2014a). Major evolutionary trends in hydrogen isotope fractionation of vascular plant leaf waxes. *PLoS One* 9, e112610. doi:10.1371/journal.pone.0112610

Gao, L., Guimond, J., Thomas, E. K., and Huang, Y. (2015). Major trends in leaf wax abundance, δ^2H and $\delta^{13}C$ values along leaf venation in five species of C_3 plants: physiological and geochemical implications. *Org. Geochem.* 78, 144–152. doi:10.1016/j.orggeochem.2014.11.005

Gao, L., Hou, J., Toney, J. L., MacDonald, D., and Huang, Y. (2011). Mathematical modeling of the aquatic macrophyte inputs of mid-chain *n*-alkyl lipids to lake sediments: implications for interpreting compound specific hydrogen isotopic records. *Geochim. Cosmoc. Acta* 75, 3781–3791. doi:10.1016/j.gca.2011.04.008

Gao, L., Zheng, M., Fraser, M., and Huang, Y. (2014b). Comparable hydrogen isotopic fractionation of plant leaf wax *n*-alkanoic acids in arid and humid subtropical ecosystems. *Geochem. Geophys. Geosystems* 15, 361–373. doi:10.1002/2013GC005015

Griepentrog, M., De Wispelaere, L., Bauters, M., Bodé, S., Hemp, A., Verschuren, D., et al. (2019). Influence of plant growth form, habitat and season on leaf-wax *n*-alkane hydrogen-isotopic signatures in equatorial East Africa. *Geochim. Cosmoc. Acta* 263, 122–139. doi:10.1016/j.gca.2019.08.004

Hajek, M., Horsak, M., Hajkova, P., and Dite, D. (2006). Habitat diversity of central European fens in relation to environmental gradients and an effort to standardise fen terminology in ecological studies. *Perspect. Plant Ecol. Evol. Syst.* 8, 97–114. doi:10.1016/j.ppees.2006.08.002

Han, J., and Calvin, M. (1969). Hydrocarbon distribution of algae and bacteria, and microbiological activity in sediments. *Proc. Natl. Acad. Sci. U. S. A.* 64, 436–443. doi:10.1073/pnas.64.2.436

He, D., Ladd, N. S., Sachs, J. P., and Jaffé, R. (2017). Inverse relationship between salinity and $^2H/^1H$ fractionation in leaf wax *n*-alkanes from Florida mangroves. *Org. Geochem.* 110, 1–12. doi:10.1016/j.orggeochem.2017.04.007

He, D., Ladd, N. S., Saunders, C. J., Mead, R. N., and Jaffé, R. (2020). Distribution of n-alkanes and their δ^2H and $\delta^{13}C$ values in typical plants along a terrestrial-coastal-oceanic gradient. *Geochim. Cosmoc. Acta* 281, 31–52. doi:10.1016/j.gca.2020.05.003

Hellenic National Meteorological Service (2018). Hellenic national meteorological Service. Available at: http://www.HNMS.gr.

Hoffmann, B., Kahmen, A., Cernusak, L. A., Arndt, S. K., and Sachse, D. (2013). Abundance and distribution of leaf wax n-alkanes in leaves of Acacia and Eucalyptus trees along a strong humidity gradient in northern Australia. *Org. Geochem.* 62, 62–67. doi:10.1016/j.orggeochem.2013.07.003

Hou, J., Andrea, W. J. D., Macdonald, D., and Huang, Y. (2007a). Hydrogen isotopic variability in leaf waxes among terrestrial and aquatic plants around Blood Pond, Massachusetts (USA). *Massachusetts* 38, 977–984. doi:10.1016/j.orggeochem.2006.12.009

Hou, J., D'Andrea, W. J., Huang, Y., D'Andrea, W. J., Huang, Y., D'Andrea, W. J., et al. (2008). Can sedimentary leaf waxes record D/H ratios of continental precipitation? Field, model, and experimental assessments. *Geochim. Cosmoc. Acta* 72, 3503–3517. doi:10.1016/j.gca.2008.04.030

Hou, J., D'Andrea, W. J., MacDonald, D., Huang, Y., D'Andrea, W. J., MacDonald, D., et al. (2007b). Hydrogen isotopic variability in leaf waxes among terrestrial and aquatic plants around Blood Pond, Massachusetts (USA). *Org. Geochem.* 38, 977–984. doi:10.1016/j.orggeochem.2006.12.009

Huang, X., and Meyers, P. A. (2019). Assessing paleohydrologic controls on the hydrogen isotope compositions of leaf wax *n*-alkanes in Chinese peat deposits. *Palaeogeogr. Palaeoclimatol. Palaeoecol.* 516, 354–363. doi:10.1016/j.palaeo.2018.12.017

Huang, X., Pancost, R. D., Xue, J., Gu, Y., Evershed, R. P., and Xie, S. (2018). Response of carbon cycle to drier conditions in the mid-Holocene in central China. *Nat. Commun.* 9, 1369–9. doi:10.1038/s41467-018-03804-w

IAEA/WMO (2017). Global network of isotopes in precipitation. GNIP Database. Available at: http://www.iaea.org/water.

Jacob, J., Bossard, N., Bariac, T., Terwilliger, V., Biron, P., Richard, P., et al. (2021). Hydrogen isotopic fractionations during syntheses of lipid biomarkers in the seeds of broomcorn millet (*Panicum miliaceum* L.) under controlled environmental conditions. *Org. Geochem.* 154, 104221. doi:10.1016/j.orggeochem.2021.104221

Jansen, B., and Wiesenberg, G. L. B. (2017). Opportunities and limitations related to the application of plant-derived lipid molecular proxies in soil science. *Soil* 3, 211–234. doi:10.5194/soil-3-211-2017

Kahmen, A., Dawson, T. E., Vieth, A., and Sachse, D. (2011). Leaf wax *n*-alkane δD values are determined early in the ontogeny of *Populus trichocarpa* leaves when grown under controlled environmental conditions. *Plant, Cell Environ.* 34, 1639–1651. doi:10.1111/j.1365-3040.2011.02360.x

Kahmen, A., Schefuß, E., and Sachse, D. (2013). Leaf water deuterium enrichment shapes leaf wax *n*-alkane δD values of angiosperm plants I: experimental evidence and mechanistic insights. *Geochim. Cosmoc. Acta* 111, 39–49. doi:10.1016/J.GCA.2012.09.003

Kahmen, A., Simonin, K., Tu, K. P., Merchant, A., Callister, A., Siegwolf, R., et al. (2008). Effects of environmental parameters, leaf physiological properties and leaf water relations on leaf water $\delta^{18}O$ enrichment in different Eucalyptus species. *Plant, Cell Environ.* 31, 738–751. doi:10.1111/j.1365-3040.2008.01784.x

Kalaitzidis, S. (2007). *Genesis and evolution of peatlands in Greece*. PhD thesis. Patras: Patras University.

Kaufman, D., McKay, N., Routson, C., Erb, M., Davis, B., Heiri, O., et al. (2020). A global database of Holocene paleotemperature records. *Sci. Data* 7, 115–134. doi:10.1038/s41597-020-0445-3

Koch, K., and Ensikat, H.-J. J. (2008). The hydrophobic coatings of plant surfaces: epicuticular wax crystals and their morphologies, crystallinity and molecular self-assembly. *Micron* 39, 759–772. doi:10.1016/j.micron.2007.11.010

Kong, D., Miao, C., Duan, Q., Lei, X., and Li, H. (2018). Vegetation-climate interactions on the Loess Plateau: a nonlinear granger causality analysis. *J. Geophys. Res. Atmos.* 123, 68–79. doi:10.1029/2018JD029036

Kottek, M., Grieser, J., Beck, C., Rudolf, B., and Rubel, F. (2006). World map of the Köppen-Geiger climate classification updated. *Meteorol. Z.* 15, 259–263. doi:10.1127/0941-2948/2006/0130

Kuhn, T. K., Krull, E. S., Bowater, A., Grice, K., and Gleixner, G. (2010). The occurrence of short chain *n*-alkanes with an even over odd predominance in higher plants and soils. *Org. Geochem.* 41, 88–95. doi:10.1016/j.orggeochem.2009.08.003

Ladd, N. S., and Sachs, J. P. (2012). Inverse relationship between salinity and *n*-alkane δD values in the mangrove *Avicennia marina*. *Org. Geochem.* 48, 25–36. doi:10.1016/j.orggeochem.2012.04.009

Ladd, S. N., Nelson, D. B., Schubert, C. J., and Dubois, N. (2018). Lipid compound classes display diverging hydrogen isotope responses in lakes along a nutrient gradient. *Geochim. Cosmoc. Acta* 237, 103–119. doi:10.1016/j.gca.2018.06.005

Lê, S., Josse, J., and Husson, F. (2008). FactoMineR: an R package for multivariate analysis. *J. Stat. Softw.* 25, 1–18. doi:10.18637/jss.v025.i01

Lionello, P., Abrantes, F. F., Gacic, M., Planton, S., Trigo, R. M., and Ulbrich, U. (2014). The climate of the Mediterranean region: research progress and climate change impacts. *Reg. Environ. Chang.* 14, 1679–1684. doi:10.1007/s10113-014-0666-0

Liu, H., Liu, Z., Zhao, C., and Liu, W. (2019a). *n*-Alkyl lipid concentrations and distributions in aquatic plants and their individual δD variations. *Sci. China Earth Sci.* 62, 1441–1452. doi:10.1007/s11430-019-9370-8

Liu, H., Wang, S., Wang, H., Cao, Y., Hu, J., and Liu, W. (2023). Apparent fractionation of hydrogen isotope from precipitation to leaf wax *n*-alkanes from natural environments and manipulation experiments. *Sci. Total Environ.* 877, 162970. doi:10.1016/j.scitotenv.2023.162970

Liu, J., and An, Z. (2018). A hierarchical framework for disentangling different controls on leaf wax δD *n*-alkane values in terrestrial higher plants. *Quat. Sci. Rev.* 201, 409–417. doi:10.1016/j.quascirev.2018.10.026

Liu, J., and An, Z. (2019). Variations in hydrogen isotopic fractionation in higher plants and sediments across different latitudes: implications for paleohydrological reconstruction. *Sci. Total Environ.* 650, 470–478. doi:10.1016/j.scitotenv.2018.09.047

Liu, J., An, Z., and Liu, H. (2018). Leaf wax *n*-alkane distributions across plant types in the central Chinese Loess Plateau. *Org. Geochem.* 125, 260–269. doi:10.1016/j.orggeochem.2018.09.006

Liu, J., An, Z., Wang, Z., and Wu, H. (2017). Using δD *n*-alkane as a proxy for paleo-environmental reconstruction: a good choice to sample at the site dominated by woods. *Sci. Total Environ.* 599–600, 554–559. doi:10.1016/j.scitotenv.2017.05.004

Liu, J., An, Z., Wu, H., and Yu, Y. (2019b). Comparison of *n*-alkane concentrations and δD values between leaves and roots in modern plants on the Chinese Loess Plateau. *Org. Geochem.* 138, 103913. doi:10.1016/j.orggeochem.2019.103913

Liu, J., Liu, W., An, Z., and Yang, H. (2016). Different hydrogen isotope fractionations during lipid formation in higher plants: implications for paleohydrology reconstruction at a global scale. *Sci. Rep.* 6, 19711–19810. doi:10.1038/srep19711

Liu, W., and Yang, H. (2008). Multiple controls for the variability of hydrogen isotopic compositions in higher plant *n*-alkanes from modern ecosystems. *Glob. Chang. Biol.* 14, 2166–2177. doi:10.1111/j.1365-2486.2008.01608.x

Liu, W., Yang, H., and Li, L. (2006). Hydrogen isotopic compositions of *n*-alkanes from terrestrial plants correlate with their ecological life forms. *Oecologia* 150, 330–338. doi:10.1007/s00442-006-0494-0

Marzi, R., Torkelson, B. E., and Olson, R. K. (1993). A revised carbon preference index. *Org. Geochem.* 20, 1303–1306. doi:10.1016/0146-6380(93)90016-5

McFarlin, J. M., Axford, Y., Masterson, A. L., and Osburn, M. R. (2019). Calibration of modern sedimentary δ^2H plant wax-water relationships in Greenland lakes. *Quat. Sci. Rev.* 225, 105978. doi:10.1016/j.quascirev.2019.105978

McNaughton, S. J. (1966). Ecotype function in the Typha community-type. *Ecol. Monogr.* 36, 297–325. doi:10.2307/1942372

Mead, R., Xu, Y., Chong, J., and Jaffé, R. (2005). Sediment and soil organic matter source assessment as revealed by the molecular distribution and carbon isotopic composition of *n*-alkanes. *Org. Geochem.* 36, 363–370. doi:10.1016/j.orggeochem.2004.10.003

Meyers, P. A. (2003). Applications of organic geochemistry to paleolimnological reconstructions: a summary of examples from the Laurentian Great Lakes. *Org. Geochem.* 34, 261–289. doi:10.1016/S0146-6380(02)00168-7

Mighall, T. M., Cortizas, A. M., Biester, H., and Turner, S. E. (2006). Proxy climate and vegetation changes during the last five millennia in NW Iberia: pollen and non-pollen palynomorph data from two ombrotrophic peat bogs in the North Western Iberian Peninsula. *Rev. Palaeobot. Palynol.* 141, 203–223. doi:10.1016/j.revpalbo.2006.03.013

Miola, A., Bondesan, A., Corain, L., Favaretto, S., Mozzi, P., Piovan, S., et al. (2006). Wetlands in the Venetian Po plain (northeastern Italy) during the last glacial maximum: interplay between vegetation, hydrology and sedimentary environment. *Rev. Palaeobot. Palynol.* 141, 53–81. doi:10.1016/j.revpalbo.2006.03.016

Moore, G. E., Burdick, D. M., Peter, C. R., and Keirstead, D. R. (2012). Belowground biomass of *Phragmites australis* in coastal marshes. *Northeast. Nat.* 19, 611–626. doi:10.1656/045.019.0406

Mulligan, G. A., Munro, D. B., and McNeill, J. (1983). The status of *Stachys palustris* (labiatae) in north America. *Can. J. Bot.* 61, 679–682. doi:10.1139/b83-077

Newberry, S. L., Kahmen, A., Dennis, P., and Grant, A. (2015). *n*-Alkane biosynthetic hydrogen isotope fractionation is not constant throughout the growing season in the riparian tree *Salix viminalis*. *Geochim. Cosmoc. Acta* 165, 75–85. doi:10.1016/j.gca.2015.05.001

Newberry, S. L., Nelson, D. B., and Kahmen, A. (2017). Cryogenic vacuum artifacts do not affect plant water - uptake studies using stable isotope analysis. *Ecohydrology* 10, 1–10. doi:10.1002/eco.1892

Nichols, J., Booth, R. K., Jackson, S. T., Pendall, E. G., and Huang, Y. (2010). Differential hydrogen isotopic ratios of *Sphagnum* and vascular plant biomarkers in ombrotrophic peatlands as a quantitative proxy for precipitation-evaporation balance. *Geochim. Cosmoc. Acta* 74, 1407–1416. doi:10.1016/j.gca.2009.11.012

Nichols, J. E., Booth, R. K., Jackson, S. T., Pendall, E. G., and Huang, Y. (2006). Paleohydrologic reconstruction based on *n*-alkane distributions in ombrotrophic peat. *Org. Geochem.* 37, 1505–1513. doi:10.1016/j.orggeochem.2006.06.020

Niedermeyer, E. M., Chase, B. M., Gleixner, G., and Mulch, A. (2016a). Southwestern African climate change during Heinrich Stadial 1 inferred from plant wax δ^{13}C and δD from rock hyrax middens. *Quat. Int.* 404, 202. doi:10.1016/j.quaint.2015.08.181

Niedermeyer, E. M., Forrest, M., Beckmann, B., Sessions, A. L., Mulch, A., and Schefuß, E. (2016b). The stable hydrogen isotopic composition of sedimentary plant waxes as quantitative proxy for rainfall in the West African Sahel. *Geochim. Cosmoc. Acta* 184, 55–70. doi:10.1016/j.gca.2016.03.034

Niedermeyer, E. M., Sessions, A. L., Feakins, S. J., and Mohtadi, M. (2014). Hydroclimate of the western indo-pacific warm pool during the past 24,000 years. *Proc. Natl. Acad. Sci.* 111, 9402–9406. doi:10.1073/pnas.1323585111

Nott, C. J., Xie, S., Avsejs, L. A., Maddy, D., Chambers, F. M., and Evershed, R. P. (2000). *n*-Alkane distributions in ombrotrophic mires as indicators of vegetation change related to climatic variation. *Org. Geochem.* 31, 231–235. doi:10.1016/S0146-6380(99)00153-9

Oakes, A. M., and Hren, M. T. (2015). Temporal variations in the δD of leaf n-alkanes from four riparian plant species. *Org. Geochem.* 97, 122–130. doi:10.1016/j.orggeochem.2016.03.010

OpenStreetMap contributors (2018). OpenStreetMap contributors. Available at: http://www.maps-for-free.com.

Pancost, R. D., Baas, M., Van Geel, B., and Sinninghe Damsté, J. S. (2002). Biomarkers as proxies for plant inputs to peats: an example from a sub-boreal ombrotrophic bog. *Org. Geochem.* 33, 675–690. doi:10.1016/S0146-6380(02)00048-7

Pedentchouk, N., Sumner, W., Tipple, B. J., Pagani, M., and Sumnerb, W. (2008). δ^{13}C and δD compositions of *n*-alkanes from modern angiosperms and conifers: an experimental set up in central Washington State, USA. *Org. Geochem.* 39, 1066–1071. doi:10.1016/j.orggeochem.2008.02.005

Peichl, M., Gažovič, M., Vermeij, I., De Goede, E., Sonnentag, O., Limpens, J., et al. (2018). Peatland vegetation composition and phenology drive the seasonal trajectory of maximum gross primary production. *Sci. Rep.* 8, 8012–8111. doi:10.1038/s41598-018-26147-4

Pérez-Angel, L. C., Sepúlveda, J., Montes, C., Smith, J. J., Molnar, P., González-Arango, C., et al. (2022). Mixed signals from the stable isotope composition of precipitation and plant waxes in the northern tropical andes. *J. Geophys. Res. Biogeosc* 127, 1–19. doi:10.1029/2022JG006932

Polissar, P. J., and D'Andrea, W. J. (2014). Uncertainty in paleohydrologic reconstructions from molecular δD values. *Geochim. Cosmoc. Acta* 129, 146–156. doi:10.1016/j.gca.2013.12.021

Pontevedra-Pombal, X., Castro, D., Souto, M., Fraga, I., Blake, W. H., Blaauw, M., et al. (2019). 10,000 years of climate control over carbon accumulation in an Iberian bog (southwestern Europe). *Geosci. Front.* 10, 1521–1533. doi:10.1016/j.gsf.2018.09.014

Post-Beittenmiller, D. (1996). Biochemistry and molecular biology of wax production in plants. *Annu. Rev. Plant Biol.* 47, 405–430. doi:10.1146/annurev.arplant.47.1.405

Poynter, J. (1989). *Molecular stratigraphy: the recognition of palaeoclimatic signals in organic geochemical data*. PhD, Sch. Chem. Bristol: University of Bristol.

Pross, J., Koutsodendris, A., Christanis, K., Fischer, T., Fletcher, W. J., Hardiman, M., et al. (2015). The 1.35-Ma-long terrestrial climate archive of Tenaghi Philippon, northeastern Greece: evolution, exploration, and perspectives for future research. *Newsletters Stratigr.* 48, 253–276. doi:10.1127/nos/2015/0063

Raeymaekers, G. (1998). Conserving mires in the European union. *Off. Off. Publ. Eur. Communities* 216, 1–96.

Rao, Z., Zhu, Z., Jia, G., Henderson, A. C. G. G., Xue, Q., Wang, S., et al. (2009). Compound specific δD values of long chain *n*-alkanes derived from terrestrial higher plants are indicative of the δD of meteoric waters: evidence from surface soils in eastern China. *Org. Geochem.* 40, 922–930. doi:10.1016/j.orggeochem.2009.04.011

Sachse, D., Billault, I., Bowen, G. J., Chikaraishi, Y., Dawson, T. E., Feakins, S. J., et al. (2012). Molecular paleohydrology: interpreting the hydrogen-isotopic composition of lipid biomarkers from photosynthesizing organisms. *Annu. Rev. Earth Planet. Sci.* 40, 221–249. doi:10.1146/annurev-earth-042711-105535

Sachse, D., Dawson, T. E., and Kahmen, A. (2015). Seasonal variation of leaf wax *n*-alkane production and δ^2H values from the evergreen oak tree, *Quercus agrifolia*. *Isot. Environ. Health Stud.* 51, 124–142. doi:10.1080/10256016.2015.1011636

Sachse, D., Gleixner, G., Wilkes, H., and Kahmen, A. (2010). Leaf wax *n*-alkane δD values of field-grown barley reflect leaf water δD values at the time of leaf formation. *Geochim. Cosmoc. Acta* 74, 6741–6750. doi:10.1016/j.gca.2010.08.033

Sachse, D., Kahmen, A., and Gleixner, G. (2009). Significant seasonal variation in the hydrogen isotopic composition of leaf-wax lipids for two deciduous tree ecosystems (*Fagus sylvativa* and *Acer pseudoplatanus*). *Org. Geochem.* 40, 732–742. doi:10.1016/j.orggeochem.2009.02.008

Sachse, D., Radke, J., Gaupp, R., Schwark, L., Lüniger, G., and Gleixner, G. (2004a). Reconstruction of palaeohydrological conditions in a lagoon during the 2nd Zechstein cycle through simultaneous use of δD values of individual n-alkanes and δ18O and δ13C values of carbonates. *Int. J. Earth Sci.* 93, 554–564. doi:10.1007/s00531-004-0408-5

Sachse, D., Radke, J., and Gleixner, G. (2004b). Hydrogen isotope ratios of recent lacustrine sedimentary *n*-alkanes record modern climate variability. *Geochim. Cosmoc. Acta* 68, 4877–4889. doi:10.1016/j.gca.2004.06.004

Sachse, D., Radke, J., and Gleixner, G. (2006). δD values of individual *n*-alkanes from terrestrial plants along a climatic gradient - implications for the sedimentary biomarker record. *Org. Geochem.* 37, 469–483. doi:10.1016/j.orggeochem.2005.12.003

Sachse, D., and Sachs, J. P. (2008). Inverse relationship between D/H fractionation in cyanobacterial lipids and salinity in Christmas Island saline ponds. *Geochim. Cosmoc. Acta* 72, 793–806. doi:10.1016/j.gca.2007.11.022

Sauer, P. E., Eglinton, T. I., Hayes, J. M., Schimmelmann, A., and Sessions, A. L. (2001). Compound-specific D/H ratios of lipid biomarkers from sediments as a proxy for environmental and climatic conditions. *Geochim. Cosmoc. Acta* 65, 213–222. doi:10.1016/S0016-7037(00)00520-2

Schefuß, E., Schouten, S., Jansen, J. H. F., and Damste, J. S. S. (2003). African vegetation controlled by tropical sea surface temperatures in the mid-Pleistocene period. *Nature* 422, 418–421. doi:10.1038/nature01500

Schemmel, F., Niedermeyer, E. M., Schwab, V. F., Gleixner, G., Pross, J., and Mulch, A. (2016). Plant wax δD values record changing Eastern Mediterranean atmospheric circulation patterns during the 8.2 kyr B. P. climatic event. *Quat. Sci. Rev.* 133, 96–107. doi:10.1016/j.quascirev.2015.12.019

Schlitzer, R. (2007). Ocean data view. Available at: http://odv.awi.de.

Schmidt, H. L., Werner, R. A., and Eisenreich, W. (2003). Systematics of ^{2}H patterns in natural compounds and its importance for the elucidation of biosynthetic pathways. *Phytochem. Rev.* 2, 61–85. doi:10.1023/B:PHYT.0000004185.92648.ae

Sessions, A. L. (2006). Seasonal changes in D/H fractionation accompanying lipid biosynthesis in *Spartina alterniflora*. *Geochim. Cosmoc. Acta* 70, 2153–2162. doi:10.1016/j.gca.2006.02.003

Sessions, A. L., Burgoyne, T. W., Schimmelmann, A., and Hayes, J. M. (1999). Fractionation of hydrogen isotopes in lipid biosynthesis. *Org. Geochem.* 30, 1193–1200. doi:10.1016/S0146-6380(99)00094-7

Shepherd, T., and Griffiths, D. W. (2006). The effects of stress on plant cuticular waxes. *New Phytol.* 171, 469–499. doi:10.1111/j.1469-8137.2006.01826.x

Shi, M., Han, J., Wang, G., Wang, J., Han, Y., and Cui, L. (2021). A long-term investigation of the variation in leaf wax *n*-alkanes responding to climate on Dongling Mountain, north China. *Quat. Int.* 592, 67–79. doi:10.1016/j.quaint.2021.04.020

Silliman, J. E., and Schelske, C. L. (2003). Saturated hydrocarbons in the sediments of lake apopka, Florida. *Org. Geochem.* 34, 253–260. doi:10.1016/S0146-6380(02)00169-9

Smith, F. A., and Freeman, K. H. (2006). Influence of physiology and climate on δD of leaf wax *n*-alkanes from C_3 and C_4 grasses. *Geochim. Cosmoc. Acta* 70, 1172–1187. doi:10.1016/j.gca.2005.11.006

Speckert, T. C., Petibon, F., and Wiesenberg, G. L. B. (2023). Late-season biosynthesis of leaf fatty acids and *n*-alkanes of a mature beech (*Fagus sylvatica*) tree traced via $^{13}CO_2$ pulse-chase labelling and compound-specific isotope analysis. *Front. Plant Sci.* 13, 1029026–1029114. doi:10.3389/fpls.2022.1029026

Srivastava, K., and Wiesenberg, G. L. B. (2018). Severe drought-influenced composition and $\delta^{13}C$ of plant and soil *n*-alkanes in model temperate grassland and heathland ecosystems. *Org. Geochem.* 116, 77–89. doi:10.1016/j.orggeochem.2017.11.002

Stefanescu, I. C., Macdonald, C., Cook, C. S., Williams, D. G., and Shuman, B. N. (2023). Mid- and long-chain leaf wax δ^2H values in modern plants and lake sediments from mid-latitude North America. *Geochim. Cosmoc. Acta* 340, 158–171. doi:10.1016/j.gca.2022.11.001

Struck, J., Bliedtner, M., Strobel, P., Schumacher, J., Bazarradnaa, E., and Zech, R. (2020). Leaf wax *n*-alkane patterns and compound-specific $\delta^{13}C$ of plants and topsoils from semi-arid and arid Mongolia. *Biogeosciences* 17, 567–580. doi:10.5194/bg-17-567-2020

Tanneberger, F., Mariné, A. M., Stanová, V. Š., and Pérez, P. H. (2017). The peatland map of Europe. *Mires Peat* 19, 1–17. doi:10.19189/MaP.2016.OMB.264

Teunissen van Manen, M. L., Jansen, B., Cuesta, F., León-Yánez, S., Gosling, W. D., Lana, M., et al. (2019). Leaf wax *n*-alkane patterns of six tropical montane tree species show species-specific environmental response. *Ecol. Evol.* 9, 9120–9128. doi:10.1002/ece3.5458

Theocharopoulos, M., Georgiadis, T., Dimitrellos, G., Chochliouros, S., and Tiniakou, A. (2006). Vegetation types with *Cladium mariscus* (Cyperaceae) in Greece. *Willdenowia* 36, 247–256. doi:10.3372/wi.36.36120

Thomas, C. L., Jansen, B., Van Loon, E. E., and Wiesenberg, G. L. B. (2021). Transformation of n-alkanes from plant to soil: a review. *Soil* 7, 785–809. doi:10.5194/soil-7-785-2021

Tierney, J. E., Pausata, F. S. R., and DeMenocal, P. B. (2017). Rainfall regimes of the green sahara. *Sci. Adv.* 3, e1601503. doi:10.1126/sciadv.1601503

Tipple, B. J., Berke, M. A., Doman, C. E., Khachaturyan, S., and Ehleringer, J. R. (2013). Leaf-wax *n*-alkanes record the plant–water environment at leaf flush. *PNAS* 110, 2659–2664. doi:10.1073/pnas.1213875110

Tipple, B. J., and Pagani, M. (2013). Environmental control on eastern broadleaf forest species' leaf wax distributions and D/H ratios. *Geochim. Cosmoc. Acta* 111, 64–77. doi:10.1016/j.gca.2012.10.042

Trin, C., Steudel, E., Naraian, R., Srivastava, J., Kalra, S. J. S., and Naraian, R. (2014). Environmental perspectives of *Phragmites australis* (cav.) Trin. Ex. Steudel. *Appl. Water Sci.* 4, 193–202. doi:10.1007/s13201-013-0142-x

Tzedakis, P. C., Hooghiemstra, H., and Pälike, H. (2006). The last 1.35 million years at Tenaghi Philippon: revised chronostratigraphy and long-term vegetation trends. *Quat. Sci. Rev.* 25, 3416–3430. doi:10.1016/j.quascirev.2006.09.002

Vilà, M., and Sardans, J. (1999). Plant competition in Mediterranean-type vegetation. *J. Veg. Sci.* 10, 281–294. doi:10.2307/3237150

Wang, Y. P., Luo, T., Zhou, X., Zhan, Z. W., Song, Z., and He, D. (2022). Inverse relationships between salinity and hydrogen isotope fractionation of *n*-alkanes in the *Aegiceras corniculatum* leaves and surface sediments from Zhanjiang mangrove estuary of China. *Chem. Geol.* 612, 121138. doi:10.1016/j.chemgeo.2022.121138

White, J. W. C., Lawrence, J. R., and Broecker, W. S. (1994). Modeling and interpreting ratios in tree rings: a test case of white pine in the northeastern United States. *Geochim. Cosmoc. Acta* 58, 851–862. doi:10.1016/0016-7037(94)90510-X

Wijmstra, T. A. (1969). Palynology of the first 30 metres of a 120 m deep section in Northern Greece. *Acta Bot. neerl.* 18, 511–527. doi:10.1111/j.1438-8677.1969.tb00591.x

Xoplaki, E., González-Rouco, J., Gyalistras, D., Luterbacher, J., Rickli, R., and Wanner, H. (2003). Interannual summer air temperature variability over Greece and its connection to the large-scale atmospheric circulation and Mediterranean SSTs 1950–1999. *Clim. Dyn.* 20, 537–554. doi:10.1007/s00382-002-0291-3

Yan, C., Zhang, Y., Zheng, M., Zhang, Y., Liu, M., Yang, T., et al. (2021). Effects of redox conditions and temperature on the degradation of *Sphagnum n*-alkanes. *Chem. Geol.* 561, 119927. doi:10.1016/j.chemgeo.2020.119927

Yang, H., and Huang, Y. (2003). Preservation of lipid hydrogen isotope ratios in Miocene lacustrine sediments and plant fossils at Clarkia, northern Idaho, USA. *Org. Geochem.* 34, 413–423. doi:10.1016/S0146-6380(02)00212-7

Yang, H., Liu, W., Leng, Q., Hren, M. T., and Pagani, M. (2011). Variation in *n*-alkane δD values from terrestrial plants at high latitude: implications for paleoclimate reconstruction. *Org. Geochem.* 42, 283–288. doi:10.1016/j.orggeochem.2011.01.006

Yang, H., Pagani, M., Briggs, D. E. G., Equiza, M. A., Jagels, R., Leng, Q., et al. (2009). Carbon and hydrogen isotope fractionation under continuous light: implications for paleoenvironmental interpretations of the High Arctic during Paleogene warming. *Oecologia* 160, 461–470. doi:10.1007/s00442-009-1321-1

Yu, X., Lü, X., Meyers, P. A., and Huang, X. (2021). Comparison of molecular distributions and carbon and hydrogen isotope compositions of *n*-alkanes from aquatic plants in shallow freshwater lakes along the middle and lower reaches of the Yangtze River, China. *Org. Geochem.* 158, 104270. doi:10.1016/j.orggeochem.2021.104270

Zhao, B., Zhang, Y., Huang, X., Qiu, R., Zhang, Z., and Meyers, P. A. (2018). Comparison of *n*-alkane molecular, carbon and hydrogen isotope compositions of different types of plants in the Dajiuhu peatland, central China. *Org. Geochem.* 124, 1–11. doi:10.1016/j.orggeochem.2018.07.008

Zhou, Y., Grice, K., Chikaraishi, Y., Stuart-Williams, H., Farquhar, G. D., and Ohkouchi, N. (2011). Temperature effect on leaf water deuterium enrichment and isotopic fractionation during leaf lipid biosynthesis: results from controlled growth of C3 and C4 land plants. *Phytochemistry* 72, 207–213. doi:10.1016/j.phytochem.2010.10.022

Zhou, Y., Grice, K., Stuart-Williams, H., Farquhar, G. D., Hocart, C. H., Lu, H., et al. (2010). Biosynthetic origin of the saw-toothed profile in $\delta^{13}C$ and δ^2H of *n*-alkanes and systematic isotopic differences between *n-iso-* and *anteiso*-alkanes in leaf waxes of land plants. *Phytochemistry* 71, 388–403. doi:10.1016/j.phytochem.2009.11.009